DETECTION OF HYPOTHALAMIC NEUROPEPTITE LEVELS INVOLVED IN APPETITE REGULATION IN ARIPIPRAZOLE TREATMENT

A THESIS SUBMITTED TO
THE GRADUATE SCHOOL OF NATURAL AND APPLIED SCIENCES
OF
MIDDLE EAST TECHNICAL UNIVERSITY

BY

SERHAT ÖZDEMİR

IN PARTIAL FULFILLMENT OF THE REQUIREMENTS
FOR
THE DEGREE OF MASTER OF SCIENCE
IN
BIOTECHNOLOGY

DECEMBER 2014

Approval of the thesis:

DETECTION OF HYPOTHALAMIC NEUROPEPTITE LEVELS INVOLVED IN APPETITE REGULATION IN ARIPIPRAZOLE TREATMENT

submitted by **SERHAT ÖZDEMİR** in partial fulfillment of the requirements for the degree of **Master of Science in Biotechnology Department, Middle East Technical University** by,

Prof. Dr. Gülbin Dural Ünver _____
Dean, Graduate School of **Natural and Applied Sciences**

Prof. Dr. Filiz Bengü Dilek _____
Head of Department, **Biotechnology**

Assoc. Prof. Dr. Tülin Yanık _____
Supervisor, **Biology Dept., METU**

Prof. Dr. Mahinur Akkaya _____
Co-Supervisor, **Chemistry Dept., METU**

Examining Committee Members:

Prof. Dr. Ufuk Gündüz _____
Biology Dept., METU

Assoc. Prof. Dr. Tülin Yanık _____
Biology Dept., METU

Assoc. Prof. Dr. Ayşegül Çetin Gözen _____
Biology Dept., METU

Assoc. Prof. Dr. Çağdaş Devrim Son _____
Biology Dept., METU

Assoc. Prof. Dr. Mehmet Ak _____
Meram Medical School, Necmettin Erbakan University

Date: 03.12.2014

I hereby declare that all information in this document has been obtained and presented in accordance with academic rules and ethical conduct. I also declare that, as required by these rules and conduct, I have fully cited and referenced all material and results that are not original to this work.

Name, Last name: SERHAT ÖZDEMİR

Signature:

ABSTRACT

DETECTION OF HYPOTHALAMIC NEUROPEPTITE LEVELS INVOLVED IN APPETITE REGULATION IN ARIPIPRAZOLE TREATMENT

Özdemir, Serhat

M.S. Department of Biotechnology

Supervisor: Assoc. Prof. Dr. Tülin Yanık

December 2014, 96 pages

Disruption or malfunctioning of neurotransmitter pathways, especially serotonergic and dopaminergic pathways are closely related to psychotic disorders such as schizophrenia. Antipsychotic medications are becoming widespread; however, in long term treatments, these drugs lead to considerable amount of weight gain as a side effect. Metformin, an antidiabetic drug, has previously been used to treat antipsychotic induced weight gain and aripiprazole has been defined as a neutral antipsychotic drug in terms of weight gain. Yet, the underlying action mechanisms of these drugs are still inadequately understood. Hypothalamic

neuropeptides releasing from arcuate nucleus (ARC) are known to be responsible for appetite and energy metabolism regulation. The aim of this study is to investigate the alteration of candidate gene expression levels of hypothalamic neuro peptides, neuropeptide Y (*NPY*) and proopiomelanocortin (*POMC*) by administration of metformin and aripiprazole to male Wistar rats for 14 weeks. We hypothesized that metformin may cause an increase in *POMC* mRNA levels and decrease in *NPY* mRNA levels while aripiprazole may act as a negative control of metformin. Our results demonstrated that *NPY* mRNA levels were significantly decreased in both metformin administered and aripiprazole coadministered group, on the other hand, *POMC* mRNA levels were unexpectedly decreased in all groups.

Key Words: Aripiprazole, Metformin, Neuropeptide Y, Proopiomelanocortin, Weight gain.

ÖZ

ARİPİPRAZOL TEDAVİSİNDE İŞTAH DÜZENLEMESİYLE İLİŞKİLİ HİPOTALAMİK NÖROPEPTİD SEVİYELERİNİN BELİRLENMESİ.

Özdemir, Serhat

Yüksek Lisans, Biyoteknoloji Bölümü

Tez Yöneticisi: Doç. Dr. Tülin Yanık

Aralık 2014, 96 sayfa

Şizofreni gibi psikotik rahatsızlıklar özellikle serotonerjik ve dopaminerjik nörotransmiter yolakların bozulması veya aksaklığı ile yakından ilişkilidir. Antipsikotik ilaçların kullanımı giderek yaygınlaşmakta fakat uzun dönemli tedavilerde bu ilaçlar yan etki olarak önemli ölçüde kilo alımına yol açmaktadır. Bir antidiyabet ilacı olan metforminin antipsikotik ilaçların sebep olduğu kilo alımını tedavi ettiği ve aripiprazolun kilo alımını etkilemeyen nötral bir antipsikotik ilaç olduğu tanımlanmış ama bu ilaçların etki mekanizması halen tam olarak anlaşılamamıştır. İştah ve enerji metabolizmasının düzenlenmesinde hipotalamusun arkuat çekirdeğinden salgılanan nöropeptidlerin sorumlu olduğu

bilinmektedir. Bu çalışmanın amacı 14 hafta boyunca metformin ve aripiprazol verilen erkek Wistar sıçanların nöropeptit Y (*NPY*) ve proopiomelanokortin (*POMC*) isimli aday hipotalamik nöropeptidlerin gen anlatım seviyelerindeki değişimlerin araştırılmasıdır. Metforminin *POMC* mRNA seviyesini yükseltmesini ve *NPY* mRNA seviyesini düşürmesini, aripiprazolun ise metforminin negatif kontrolü olarak etki gösterebileceğini hipotez etmekteyiz. Elde ettiğimiz sonuçlar hem sadece metformin verilen hem de aripiprazol ile birlikte verilen gruplarda *NPY* mRNA seviyesinin anlamlı biçimde düştüğünü öte yandan *POMC* mRNA seviyesinin de beklenmedik şekilde düştüğünü göstermiştir.

Anahtar Kelimeler: Aripiprazol, Metformin, Nöropeptit Y, Proopiomelanokortin, Kilo alımı.

To my family and friends

ACKNOWLEDGEMENTS

First of all, I would like to express my gratitude to my thesis advisor Assoc. Prof. Dr. Tülin Yanık for giving me an opportunity to do research in her laboratory. Moreover, I appreciate for her unlimited support, guidance, and supervision. I would also like to thank to my coadvisor Prof. Dr. Mahinur Akkaya for her support throughout my thesis period. I am also grateful to Assoc. Prof. Dr. Mehmet Ak for his contributions and guidance to this study.

Secondly, I would like to thank to my examination committee, Prof. Dr. Ufuk Gündüz, Assoc. Prof. Ayşegül Çetin Gözen, and Assoc. Prof. Dr. Çağdaş Devrim Son for reading my thesis and their valuable suggestions on this study.

I was very fortunate to have Gizem Kurt for her countless help and guidance. Additionally, I am thankful to my other laboratory mates Hikmet Taner Teker, Feride Kaşıkçı, and Barış Ulum for their help and supports. Furhermore, I am grateful for all the help and support of our enthusiastic undergraduate students, Müge Sak and Bilge Büyükdemirtaş. Also I would like to thank to our senior students Seher Koşar and Abdulahad Bayraktar for their assistance.

I would like to thank Middle East Technical University Scientific Research Coordinatorship (METU-BAP) and Gülhane Military Medical Academy (GATA) for financially supporting the project through BAP-08-11-2012-015 collaborative grant.

I am truly happy to have such brilliant friends Maryam Parsian and Emmanuel Kyere. They always guided me with their motivational speeches.

I got the opportunity to know wonderful people during my dormitory residence time. I am blissed to have Sina Khoshsima and Orhan Ata Bayman for their endless support and friendship.

With no doubt, the biggest appreciation belongs to my family, Erol Özdemir and Makbule Özdemir. I am extraordinarily lucky to have their never ending love and infinite support.

TABLE OF CONTENTS

LIST OF TABLES

TABLES

LIST OF FIGURES

FIGURES

LIST OF ABBREVIATIONS

5-HT	5-hydroxytryptamine (serotonin)
5-HT1B	Serotonin 1B receptors
5-HT2C	Serotonin 2C receptors
α-MSH	Alpha-melanocyte stimulating hormone
AAP	Atypical antipsychotic
ACC	Acetyl-CoA carboxylase
ACTH	Adrenocorticotropic hormone
AgRP	Agouti-related peptide
AMPK	Adenosine monophosphate-activated protein kinase
ANOVA	Analysis of variance
ARC	Arcuate nucleus
BBB	Blood-brain barrier
BMI	Body mass index
cDNA	Complementary DNA
cAMP	Cyclic adenosine monophosphate
CART	Cocaine and amphetamine-regulated transcript
CRD	Cytokine receptor domain
CNS	Central nervous system
D	Dopamine receptor
DEPC	Diethylpyrocarbonate
DMH	Dorsomedial hypothalamus
EDTA	Ethylenediaminetetraacetic acid

Fn3	Fibronectin III domain
GABA	Γ-Amino Butyric Acid
GAPDH	Glyceraldehyde 3-phosphate dehydrogenase
gDNA	Genomic DNA
HFD	High-fat diet
ICV	Intracerebroventricular
Ig	Immunoglobulin
InsR	Insulin receptor
IRS	Insulin receptor substrate
JAK	Janus kinase
JP	Joining peptide
LepR-B	Leptin receptor isoform b
LH	Lateral hypothalamus
MCR	Melanocortin receptor
mTOR	Mammalian target of Rapamycin
NPY	Neuropeptide Y
OECD	Organization for Economic Cooperation and Development
PBS	Phosphate buffer saline
PKA	Protein kinase A
PKC	Protein kinase C
POMC	Proopiomelanocortin
PVN	Periventricular nucleus
qRT-PCR	Quantitative real-time polymerase chain reaction
SEM	Standard error mean
SERT	Serotonin reuptake transporters
SNP	Single nucleotide polymorphism
SOCS	Suppressor of cytokine signaling
STAT	Signal transducer and activator of transcription

T2D	Type 2 diabetes
UV	Ultraviolet
VTA	Ventral tegmental area
WC	Waist circumference
WHR	Waist-hip ratio
WHO	World health organization

CHAPTER 1

INTRODUCTION

1.1 OBESITY AND BODY WEIGHT REGULATION

1.1.1 Obesity

Throughout the world, obesity is one of the most prevalent complex disorder which represents excess storage of body fat accumulation. Due to the imbalance between energy intake and expenditure, obesity leads to several serious medical conditions in the long term. For instance, among the obese adults nearly 80% of them have at least one and 40% have two or more comorbidities involving diabetes mellitus, hypertension, cardiovascular diseases and particular cancer types (Mantzoros & Flier, 2000).

In the past, obesity was common among the high-income countries; however, it is now independent from income status. According to World Health Organization (WHO) the prevalence of worldwide obesity has almost doubled since 1980. Besides, the Organization for Economic Cooperation and Development (OECD) 2014 obesity report indicates that 18% of adult population and one in five children are overweight or obese. Nowadays, about 3.4 million deaths per year can be attributed to obesity which is increasing in a gradual manner (Muennig *et al*., 2006).

Body mass index (BMI), or Quetelet index is frequently used for classification of the degree of obesity. It is described as the individual's body weight divided by the square of the height (kg/m^2) (Eknoyan, 2007). The classification of adult obesity is represented on Table 1.1.

Table 1-1 Adult obesity classifications in terms of Body Mass Index (BMI)

Category	**BMI (kg/m^2)**
Underweight	<18.50
Normal range	18.50 - 24.99
Overweight	≥25.00
Obese class I	30.00 – 34.99
Obese class II	35.00 – 39.99
Obese class III	≥40.00

Alternatively, visceral or abdominal fat mass can also be measured by according to waist to hip ratio (WHR) and waist circumference (WC) calculations which are independent of height and muscle mass. Currently, these measurements are applied in order to predict body fat and health risks (Folsom *et al*., 2000). Moreover, as compared to BMI, WC and WHR displayed remarkable association with myocardial infarction (Welborn *et al*., 2003).

1.1.1.1 Etiology

The etiology of obesity depends on several factors such as, environmental, behavioral, physiological, genetic, and cultural factors. The contributions of these factors result in energy imbalance and elevate excessive fat storage. Environmental and behavioral factors for instance, sedentary lifestyles along with excess energy intake are the main reasons account for the powerful increase in obesity throughout the past 2 decades (WHO Report, 1998).

Most of the time, the genetic aspects of obesity is not a single-gene defect, in fact it is the result of polygenic factors in both humans and animals. Recently, more than 300 genes or gene markers which are related to etiology of obesity were identified (Chagnon *et al*., 2003). Twin studies play a crucial role in terms of the genetic factors of obesity in human population. 53 twin pairs were studied in multiple countries and it has been reported that the heritability of body mass index was changing between 50% and 70% (Allison *et al*., 1996). According to the recent findings, obesity is also associated with single nucleotide polymorphisms (SNP's) (Andreasen *et al*., 2008; Frayling *et al*., 2007; Haupt *et al*., 2008).

1.1.1.2 Treatment

Recommended obesity treatment method generally depends on the patient's BMI and also whether the presence of one or more associated comorbidities. Treatment options based on BMI values are represented on Fig. 1.1.

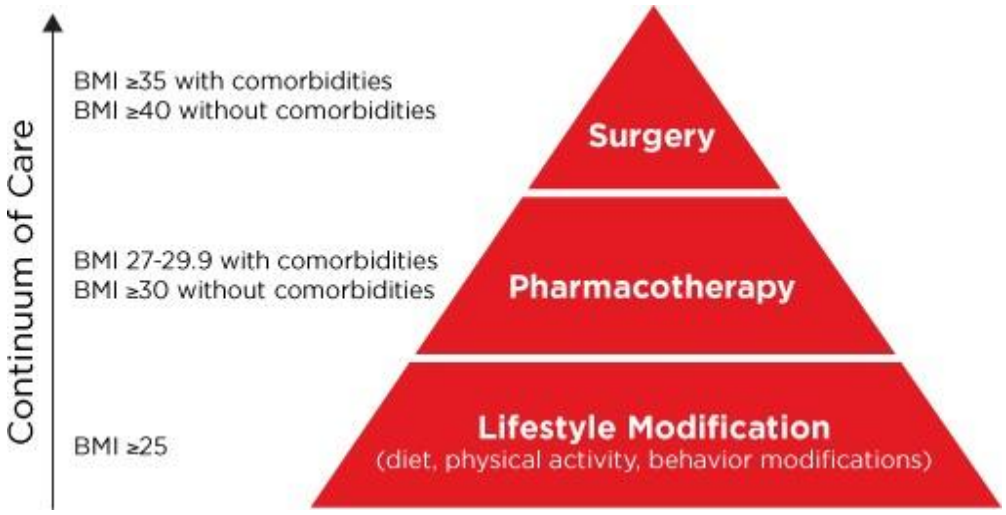

Figure 1-1 Treatment options according to BMI values.

Briefly, for patients who have a BMI of ≥25, exercise, diet, and behavior modification are advised. Patients with a BMI of ≥27 with comorbidities or BMI of ≥30 without comorbidities, pharmacotherapy is the recommended type of treatment. Furthermore, metabolic surgery is advisable for the patients who have a BMI of ≥35 with comorbidities or a BMI of ≥40 without comorbidities (Chambers *et al*., 2011).

1.2 REGULATION OF APPETITE MECHANISM

The brain regulates energy homeostasis, by adjusting a variety of nutritional signals which is a considerably complex process including many brain regions such as cortex, brainstem etc. However, hypothalamus is the most important part in terms of regulating appetite mechanism. In feeding control, the function of hypothalamus has been emerged by experiments and some of the nuclei have been indicated as satiety

and feeding centers. One of the main feeding control centers of hypothalamus is arcuate nucleus (ARC) where hormonal signals are being synthesized and secreted (Funahashi *et al*., 2000). The ARC locates above the median eminence which is a significant permeable area of the blood brain barrier (BBB). It allows the entry of the proteins and peripheral peptides such as leptin and insulin that are known to be fat mass signals (Friedman & Halaas, 1998). ARC location of the human brain is depicted on Fig. 1.2.

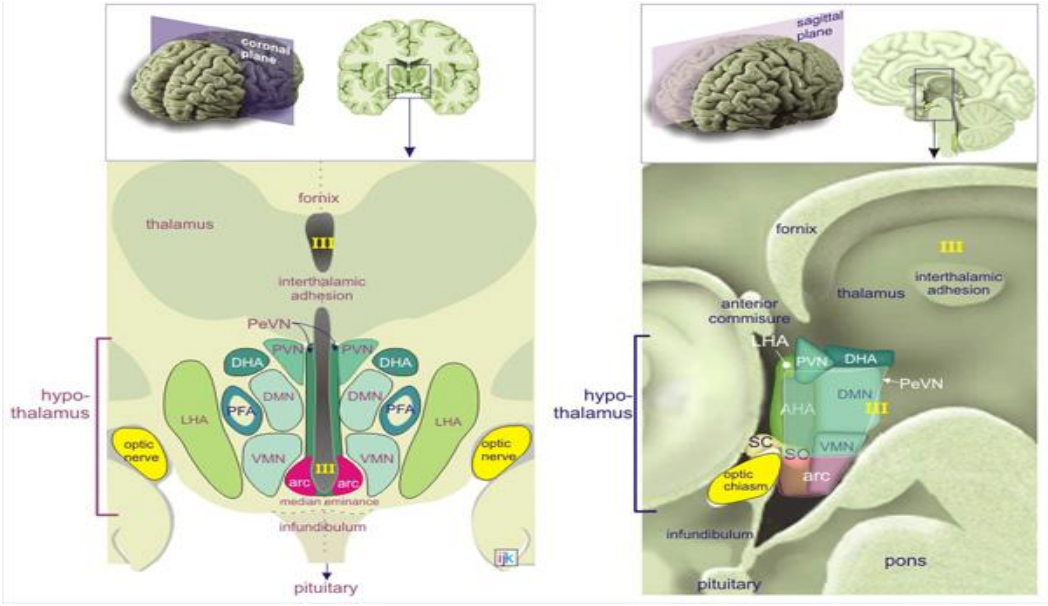

Figure 1-2 The arcuate nucleus and the neighboring hypothalamic nuclei locations of the human brain (Peyron *et al*., 2000).

1.2.1 Leptin

Leptin is a protein that contains a signal sequence and appropriate cleavage of this sequence leads to the mature form of the hormone about 16 kDa molecular weight (Zhang *et al*., 1994). According to the initial studies, white adipose tissue was the only place of leptin synthesis; however recent studies demonstrate that it is synthesized in also many other places such as placenta, stomach, brown adipose tissue, ovarian follicles, bone, heart and even possibly the brain (Trayhurn *et al*., 2001). The absence of circulating leptin due to *ob* gene mutation leads to the hyperphagic obese *ob*/*ob* mouse phenotypes. Yet, leptin administration can be the solution (Campfield *et al*., 1995). In a similar manner, mutations leading the disruption of leptin synthesis cause severe obesity in humans that can be cured by recombinant leptin treatment in adults and children (Licinio *et al*., 2004).

There are many splice variants of leptin receptors belonging to the cytokine receptors superfamily in the JAK-STAT signalling pathway (Fig. 1.3). Among these receptors, the long intracellular domain of the Ob-Rb receptor is required for the leptin's appetite function (Lee *et al*., 1996). Obese mice that have mutant Ob-Rb intracellular domain are not able to carry out JAK-STAT signaling pathway (Meister, 2000). Leptin is secreted into the circulation and it correlates with the total body fat amount (Maffei *et al*., 1995) by stimulating energy expenditure and inhibiting food intake.

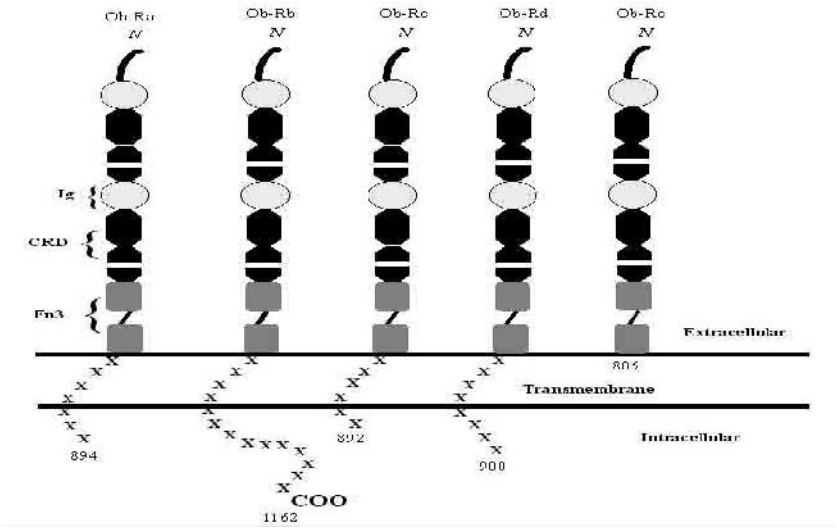

Figure 1-3 Leptin receptor isoforms. All isoforms have identical extracellular ligand binding domains but they diverge at the C terminus (Ceddia *et al*., 2001).

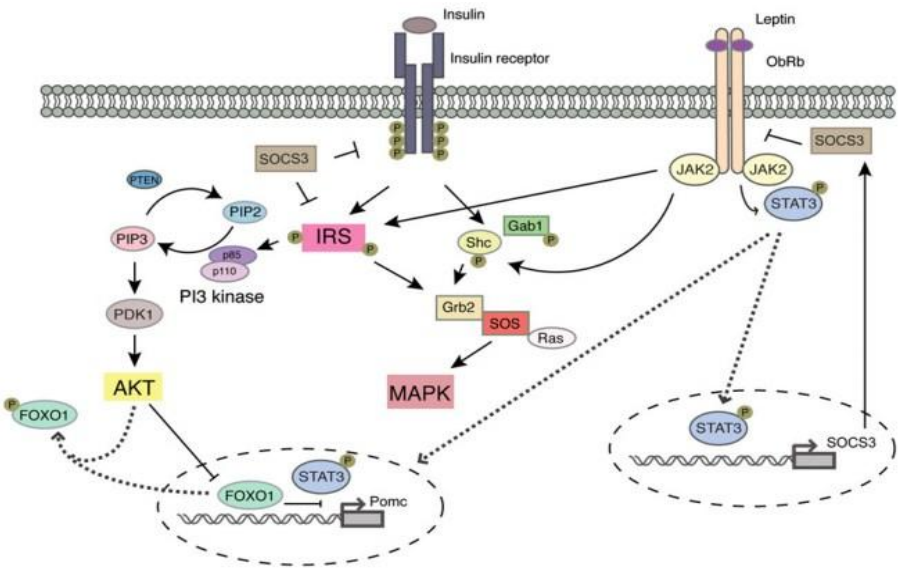

Figure 1-4 Leptin and Insulin signaling pathway (Könner & Brüning, 2012).

When leptin binds to the ObRb, it results in Janus kinase (JAK) 2 activation. JAK phosphorylates ObRb that activates STAT 3 molecules (Vaisse *et al*., 1996). Active STAT 3 forms dimers that transfer to the nucleus, and leads to the subsequent activation of suppressor of cytokine signaling (SOCS) 3. Elevated SOCS 3 expression causes leptin and insulin feedback inhibition. In addition, phosphorylated JAK 2 initiates the IRS/PI3 kinase signaling pathway, resulting in serine/threonine kinases activation (Niswender *et al*., 2001). Leptin and insulin signaling pathway is represented in Fig. 1.4. The appropriate regulation of glucose and energy homeostasis has been discovered to be required for both of these pathways' activation (Bates *et al*., 2003).

1.2.2 Hypothalamic Neuropeptides

1.2.2.1 Neuropeptide Y (*NPY*)

Neuropeptide Y (*NPY*) is one of the most abundant and widely distributed peptides of the hypothalamus. It has 36 amino acids, containing a tyrosine ('Y') at each end (Williams *et al*., 2000). It plays significant roles in neuroendocrine axes control, feeding behavior, memory retention and cardiovascular regulation (Pedrazzini, 2004). Moreover, the hypothalamic *NPY* expression takes place in ARC and after central administration its most considerable effect is the feeding stimulation (Inui, 2000). It has been previously discovered that intracerebroventricular (ICV) *NPY* administration in rats led to a strong and prolonged food intake increase (Clark *et al*., 1984). On the other hand, chronically administration of *NPY* caused obesity and hyperphagia (Stanley *et al*., 1986). Additionally, *NPY* expression levels in the hypothalamus have been detected to be upregulated with respect to control groups in several distinct rodent experiments (Wilding *et al*., 1993). Recently, five of the G-protein coupled *NPY* receptors (Y1, Y2, Y4, Y5 and Y6) have been discovered and they act as either reducing adenylate cyclase levels or enhancing intracellular

calcium levels in hypothalamus (Gehlert, 2004). The Y5 receptor has been found to be expressed at comparatively high levels in the lateral hypothalamus (LH), close to the area where *NPY* stimulates feeding most potently (Williams *et al*., 2000). During food deprivation, *NPY* secretion has been found to be increased (Kalra *et al*., 1991). In the ARC, production and secretion of *NPY* into the periventricular nucleus (PVN) are mainly regulated by inhibitory signals like insulin, leptin, and stimulatory signals such as glucocorticoids. Consequently, *NPY*'s primary physiological role might be the regulation of body fat stores and energy balance under energy deficient conditions.

1.2.2.2 Pro-opiomelanocortin (*POMC*)

POMC neurons are playing significant roles for regulating normal feeding behavior and energy homeostasis (Morton *et al*., 2006). Pharmacological and genetic experiments have demonstrated that *POMC* neurons caused energy expenditure enhancement and appetite reduction. Disruption of *POMC* neurons or mutating of the gene has led to obesity in both humans and rodents (Gropp *et al*., 2005; Xu *et al*., 2005). *POMC* neurons are mainly located in the ARC in the adult rodent brain (Padilla *et al*., 2012). According to a recent study, *POMC* neurons in the ARC stimulated optogenetically for 2 h which did not cause food intake inhibition (Aponte *et al*., 2011), suggesting that there might be additional neuronal populations playing roles in the regulation of melanocortin signaling pathway.

Five melanocortin receptors (MCRs) have been discovered in the genomes of bony fishes, cartilaginous fishes, and tetrapods (Cone, 2006). This receptor gene family was first identified for mammals, and the receptor genes were named according to the order of discovery (Gantz & Fong, 2003) represented in Fig. 1.5.

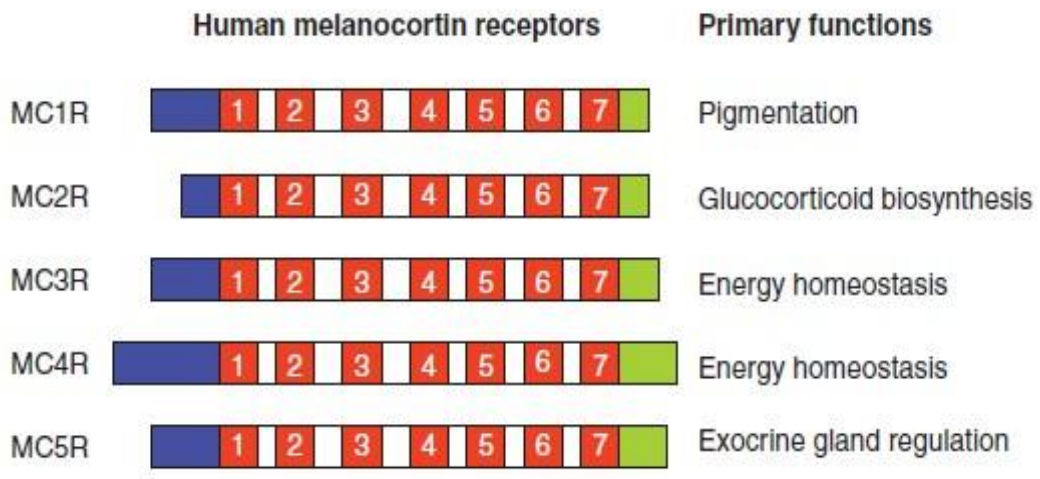

Figure 1-5 Schematic representation of human melanocortin receptors (MCRs). Transmembrane-spanning domains (red numbered boxes), N-terminal domains (blue boxes), and the C-terminal domains are depicted (green boxes) for each receptor (Gantz & Fong, 2003).

So far, MCR genes have been detected only in the chordates' genomes (Vastermark & Schiöth, 2011). The melanocortin peptides' precursor protein *POMC* encodes multiple ligands with the melanocortin core sequence (HFRW), such as ACTH, α-MSH, β-MSH, and γ-MSH (Dores & Lecaude, 2005).

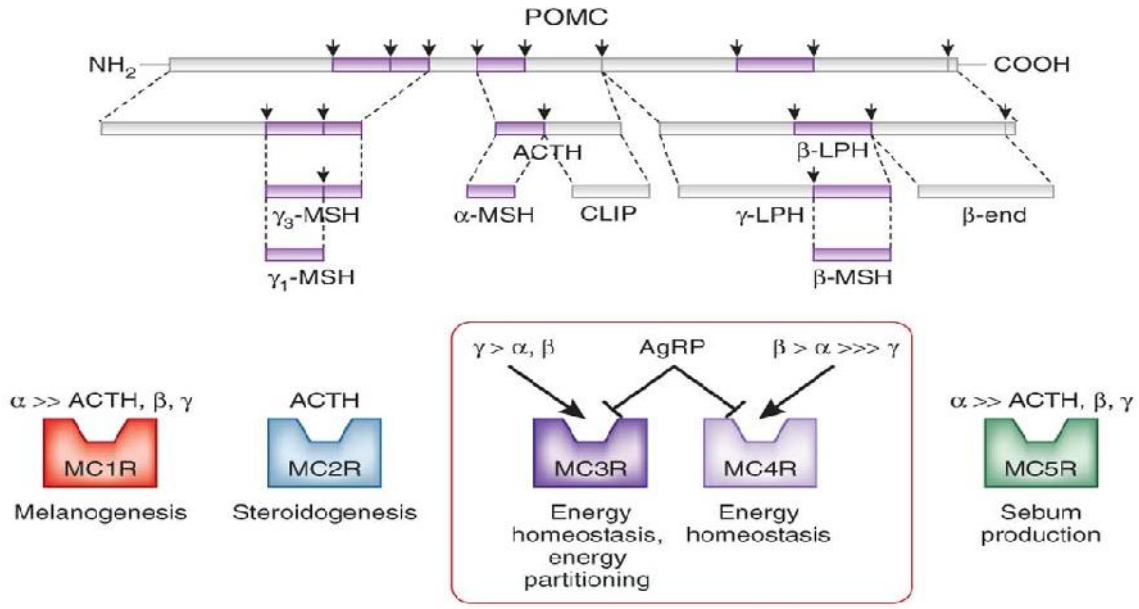

Figure 1-6 Schematic representation of *POMC* cleavage and it's receptors. Top: Post-translational modification of *POMC* to generate biologically active peptides, involving α-, β-, γ-melanocyte-stimulating hormone (MSH) and adrenocorticotropin (ACTH). Arrows represent cleavage sites. Bottom: five melanocortin receptors (MC1R–MC5R). (Yeo & Heisler, 2012).

More than 5% of the morbid obesity cases in humans are related with mutations of the MC4R gene. Heterozygous mutations resulting in severe obesity, hyperphagia, hyperinsulinemia, elevated fat mass and linear growth acceleration, whereas homozygous mutations cause an even more severe phenotype (Farooqi *et al*., 2003).

MC3R gene mutation which is responsible for obesity and insulin resistance has been detected in a child and father (Lee *et al*., 2002).

1.3 SEROTONERGIC AND DOPAMINERGIC PATHWAYS

Serotonin is associated with satiety (Halford *et al*., 2011; Williams & Elmquist, 2012) which involves three different neuron types and each one expresses distinct serotonin receptors.

Initially, serotonergic drugs acting mechanism is achieved through serotonin 2c (5-HT2C) receptor activation on *POMC* neurons (Sohn *et al*., 2011). Increasing the *POMC* neurons' firing rate led to melanocortins (MCs) release and MC4 receptors activation is also found to be involved in serotonin's mediation effect on *POMC* (Lam *et al*., 2007). It has been reported that MC4 receptor mutations induced obesity in both humans and mice (Yeo & Heisler, 2012).

Secondly, serotonin's satiating effects are also occured via 5-HT1b receptor expression on *NPY* neurons. *NPY/AgRP* neurons have optogenetically stimulated indicating the significance of food intake, furthermore, serotonin would reduce food intake by decreasing these neurons activity (Atasoy, 2012).

Finally, in the brain stem, serotonergic neurons have also been discovered to affect food intake (Wu *et al*., 2012).

According to a study, dopamine D1 receptor stimulation caused food intake enhancement, while D2 receptor stimulation led to food intake reduction (Cooper, 2006). D2 antagonist treatment resulted in weight gain implying that in the long term, D2 receptor stimulation suppresses food intake (Palmiter, 2007). Also dopamine increased *POMC* expression in the ARC and subsequently resulting decreased food intake via the lateral and ventromedial hypothalamus (Tong & Pelletier, 1992).

1.4 METFORMIN

Metformin is one of the most commonly prescribed insulin sensitizer for type 2 diabetes (T2D) treatment management. The primary target is the liver, yet metformin acts on several different tissues such as endothelium, adipose tissue, and skeletal muscles.

5'-AMP-activated protein kinase (AMPK) stimulation has previously been stated to be crucial for metformin's hepatic lipogenesis and gluconeogenesis actions (Fujii *et al*., 2006). According to some studies, metformin can decrease body weights of not only T2D patients, but also non-diabetic obese individuals (Rasouli *et al*., 2007). Metformin can also leads to a decrease in weight gain, induced by antipsychotic agents (Morrison *et al*., 2002) however, it has also been declared that metformin treatment did not improve antipsychotic induced weight gain (Baptista *et al*., 2006). In obese mice, the amount of hepatic lipids was also reduced by metformin administration (Lin *et al*., 2000). Therefore, understanding metformin's molecular basis on lipid and glucose homeostasis is crucial for improving therapeutic approaches to obesity and TD2.

Briefly, metformin's action mechanism is associated with the adjustment of cells' energy metabolism. Metformin lowers glucose levels by hepatic gluconeogenesis inhibition. In response to glucagon, mitochondrial complex I inhibition leads to abnormal protein kinase A and cAMP signaling. Metformin's proposed mode of action (Pernicova & Korbonits, 2014) is shown in Fig. 1.7.

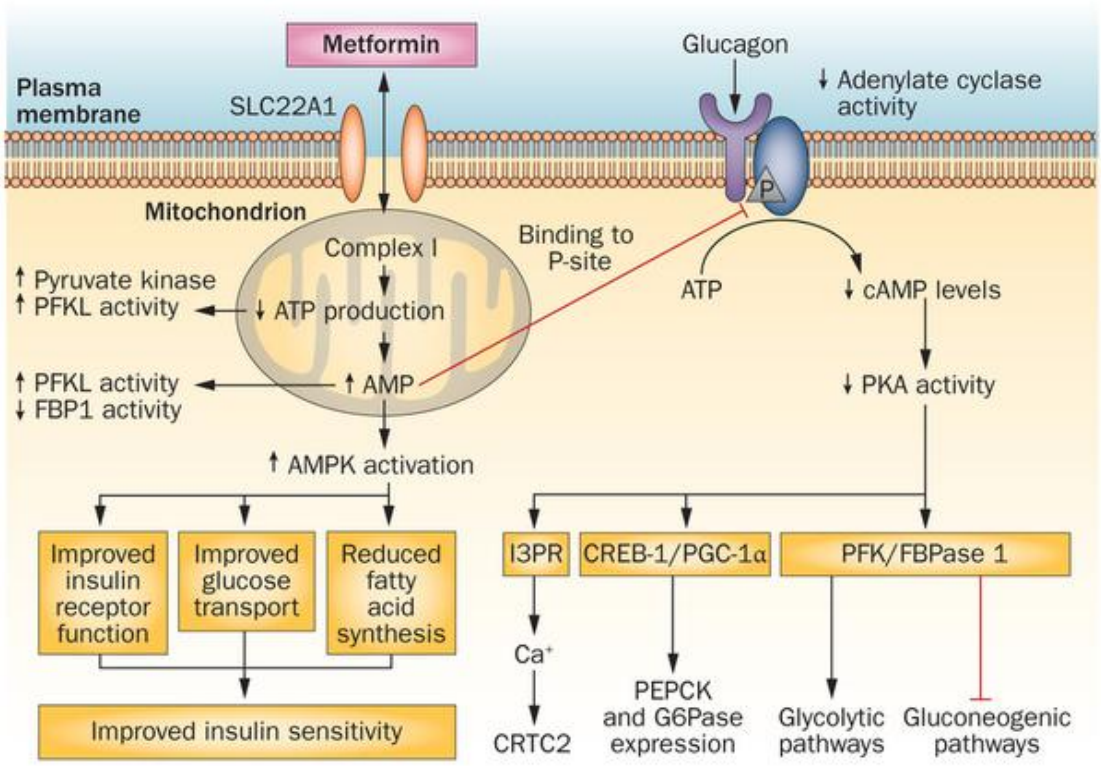

Figure 1-7 Metformin mode of action (Pernicova & Korbonits, 2014).

.

1.5 ARIPIPRAZOLE

Atypical antipsychotic (AAP) drugs have been preferred more and more by the patients for the psychotic disorders' management. Recently, it has been thought that AAP medications usage might be associated to critical adverse effects, involving glucose intolerance, hyperlipidemia and weight gain (Newcomer, 2005). 78.8% of patients who received antipsychotic agents have been reported that more than 7% of their weight increased (Alvarez *et al.*, 2006). Clinical studies demonstrate that AAP drugs might have higher potentials in terms of weight gain induction with respect to

conventional antipsychotic drugs. Amongst other antipsychotic agents, aripiprazole is the only approved antipsychotic that decreases dopaminergic neurotransmission through D2 partial agonism, not D2 antagonism. According to some aripiprazole studies, patients who have a high BMI lost weight, while having a low BMI led to weight gain, and the ones with a moderate BMI displayed little changes of weight (Chue, 2004). AAP drugs' underlying mechanism of weight gain has not been properly understood yet. However, combinations of biological, psychological and environmental factors most probably play significant roles in weight gain.

1.6 AIM OF THE STUDY

It might be possible that loss of body weight or prevention of weight gain could be performed by metformin and aripiprazole actions on *NPY* and *POMC* neurons in the ARC. Based on our knowledge, no direct rat research conducted to prove this hypothesis. Therefore**,** the aim of the study was to investigate the alteration of candidate gene expression levels of hypothalamic neuro peptides, neuropeptide Y (*NPY*) and proopiomelanocortin (*POMC*) after administration of metformin and aripiprazole to male Wistar rats for 14 weeks. We hypothesized that Metformin may cause an increase in *POMC* mRNA levels and decrease in *NPY* mRNA levels while aripiprazole may have a moderate effect on these hypothalamic neuropeptides' mRNA levels.

CHAPTER 2

MATERIALS AND METHODS

2.1 RAT STUDIES

Four weeks old 40 male Wistar rats were obtained from KOBAY (Ankara, Turkey) and randomly divided into 4 groups. The groups were named as sucrose administered group (Control 1; CTRL 1), metformin administered group (Control 2; CTRL 2), aripiprazole administered group (ARIP 1), and 7 weeks Metformin, 7 weeks aripiprazole administered group (ARIP 2). The rats were housed as 3 or 4 animals per cage under 12 hour light/dark cycle starting from 7:30 am to 7:30 pm with 22 $\pm$ 2^{o}C and a humidity of 60%. Tap water and 200 g/day/cage regular chow diet were provided *ad libitum*.

2.1.1 Preparation and Administration of Metformine and Aripiprazole

Metformin was purchased as METFULL 1000 mg effervescent tablets (Vitalis, Turkey) and aripiprazole was a gift (Aris, Turkey). Metformin tablets were dissolved in drinking water (METFULL tablet prospectus) and since it is highly soluble at pH 6.8 (Block *et al*., 2008), the final pH of the water was set to 6.8 with 4M NaOH

solution. Drugs were administered orally by using syringes (Fig. 2.2) in order to reduce stress levels in animals (Schleimer *et al*., 2005). The control group rats were received 1 ml of 10% sucrose solution twice a day. Metformin and aripiprazole were administered within drinking water 250 mg/kg in a day. Fourteen weeks of drug administration scheme was shown in Figure 2.1. Cage number and rat number were identified as "C#R#" by means "C#" represents cage number and "R#" represents rat number. Rat IDs' were indicated in Table E.1

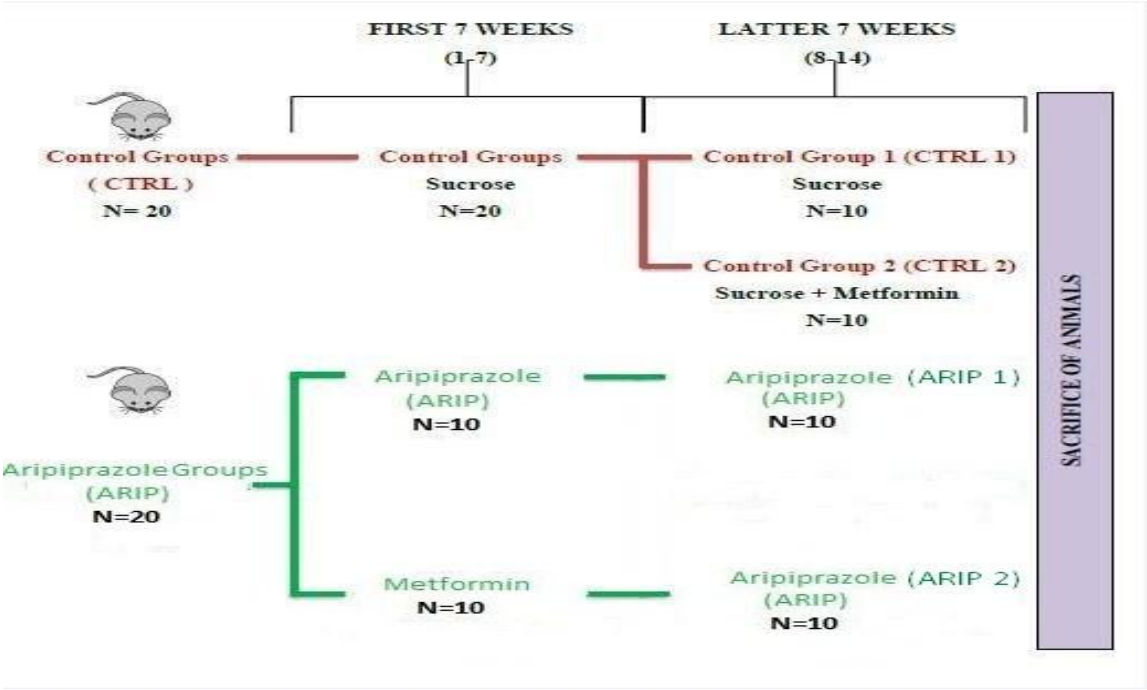

Figure 2-1 Drug administrations to the rats in 14-week time period.

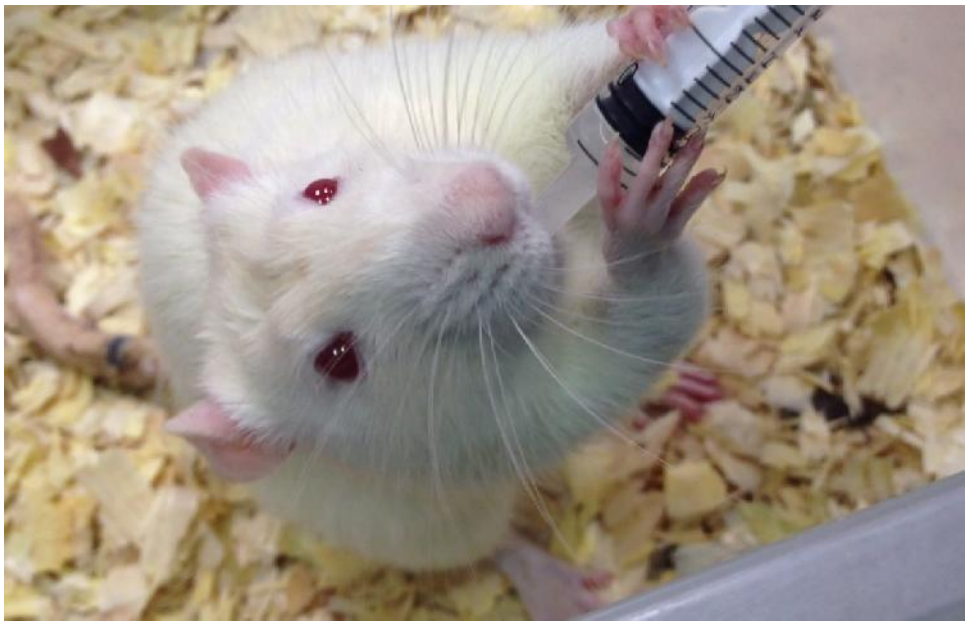

Figure 2-2 The administration way of drugs to rats.

2.1.2 Weight Gain and Food Consumption Analysis

All animals were weighed every week. Food consumption was calculated such that after 200 g regular chow diet supplied for each cage, the remaining food amount was weighed and recorded every following day around 6 pm. Difference between these amounts indicated that how much meal was consumed per cage. The slope of the trend lines were also plotted to analyze food consumption amounts of the control and experimental groups (Fig. 3.3).

2.1.3 Hypothalamus Extraction

All of the equipments (forceps, scissors, tubes etc.) required for the operation were treated with diethylpyrocarbonate (DEPC) for 16 h and then autoclaved. DEPC (Sigma-Aldrich, Germany) was prepared as in 1 ml of DEPC per 1 L of dH_2O. Also benches and micropipettes were sterilized with RNase Away (Thermo Scientific, USA) solution. At the end of 14^{th} week, the rats were sacrificed by using a guillotine. Before the sacrification process animals were exposed to 10 sec of CO_2 treatment to avoid stress related peptides' expression changes. After the complete removal of rat brains, hypothalami were extracted and washed with 1X phosphate buffer saline (PBS) (Sigma Aldrich, Germany). Afterwards hypothalami were incubated in 500 µl of RNA*later*, RNA stabilization reagent (Qiagen, Germany) and stored at -80^0C until RNA isolation.

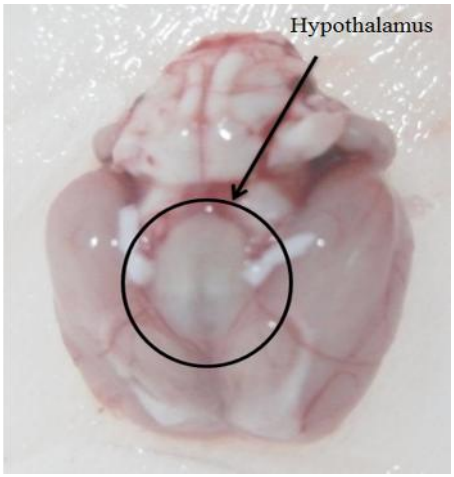

Figure 2-3 The dissected rat brain. The black circle represents the location of hypothalamus.

2.1.4 Blood and Serum Collection

Rats' trunk blood was collected into EDTA tubes and centrifuged (Selecta Centrofriger BL-II) at 1600 x *g* for 10 min. Serum samples were collected and aliquoted into sterile 1.5 ml centrifuge tubes and stored at -80^{0}C.

2.1.5 Triglyceride Quantification

Serum triglyceride concentrations were calculated by using Abcam Triglyceride Quantification Kit (USA) according to manufacturers´ instructions. In the assay, lipase hydrolyzes triglyceride ester bond which results in formation of fatty acids and glycerol. After that glycerol is phosphorylated and oxidized, generating hydrogen peroxide that reacts with the kit's colorimetric probe (absorbance of 570 nm). For this experiment, 96-well plates (Corning, USA) were used and the standard curves were formed. The samples were tested as in triplicates (n=3) and negative controls (without lipase) were used to discard glycerol background.

2.1.6 Leptin Quantification

Serum leptin levels were calculated by using mouse/rat enzyme-linked immune absorbent assay (ELISA) kit (R&D Systems, Inc., USA). In the first step of the experiment, 50µL/well assay diluent was added to each well. Standards, controls and samples (1:10 dilution) were prepared and loaded as duplicates (50µL/well) and incubated for 2 hours at RT. At the end of incubation, wells were washed 5 times with 400 µL wash buffer. 100 µL of mouse/rat leptin conjugate was added to each

well and incubated for 2 hours at RT. Wash step was repeated and 100 µL of substrate solution was added to each well. Light exposure was prevented during 30 min. of incubation at RT. As a final step, 100 µL of stop solution was added to each well and optic density was determined at 450 nm wavelength. Leptin standard curve was used for the serum leptin quantification.

2.1.7 Total RNA and Protein Isolation

Hypothalamic tissues were taken from -80^{0}C and 1 ml of 1X PBS solution was added to the tissues. In order to remove RNA*later* remnants, centrifugation was done at 10000 x *g* for 40 sec. After that tissues were taken into a new microcentrifuge tube and 1 ml TRI Reagent (Sigma Aldrich, Germany) was added on ice. Tissues were homogenized by using a drill at 2500 rpm in glass-teflon homogenizators on ice. After 10 min room temperature (RT) incubation, centrifugation was performed at 12000 x *g* for 10 min. The supernatant was taken into a new microcentrifuge tube and 200 µl ice-cold choloroform (Sigma Aldrich, Germany) was added and mixed by inversions for 30 sec. The samples were incubated for 3 min at RT then, centrifuged at 12000 x *g* for 15 min at 4^{0}C. Three phases (RNA in the upper phase, DNA in the interphase and proteins in the lower phase) were obtained. The lower protein phase was carefully collected and stored at -80^{0}C for further analyses. The upper RNA phase was gently taken into a new microcentrifuge tube then, 200 µl ice-cold choloroform was added and followed by 30 sec inversion and 7 min RT incubation. After 12000 x *g*, 15 min centrifugation process, again aqueous upper RNA phase was taken into another microcentrifuge tube and 500 µl ice-cold isopropanol (Sigma Aldrich, Germany) was added and slowly inverted. Afterwards, 1 ml glycogen (Sigma Aldrich, Germany) was added to increase RNA precipitation. The samples were incubated at -20^{0}C for 40 min. At the end of the incubation they were centrifuged at 12000 x *g* for 25 min. The supernatant was discarded and washed with

1 ml 75% ice-cold ethanol (Sigma Aldrich, Germany) and inverted in a gentle manner until the pellet is moving. Then, samples were centrifuged 7500 x *g* for 5 min and ethanol was evaporated with the help of a Bunsen burner. The pellet was dissolved in 40 µl nuclease free water (Thermo Scientific, USA). Subsequently, the RNA sample concentrations were calculated by loading 2 µl RNA sample to NanoDrop2000 (Thermo Scientific, US).

2.1.8 DNase-I Treatment and Purification of RNA Samples

The presence of genomic DNA is an undesired product and negatively affects total RNA purity; therefore DNase treatment (Ambion DNA-free Kit, USA) was performed to get rid of DNA contaminants from RNA samples. According to manufactures protocol, 10 µg of each RNA sample was taken and diluted to 44 µl of final volume. After that, 5 µl DNase I buffer and 1 µl DNase I enzyme was added to each sample and incubation was performed at 37^0C for 1 hr by using microcentrifuge tube heater (Thermoline Scientific DMB 2, Australia). Subsequently, 5 µl DNase inactivation reagent was added and samples were incubated for 2 min at RT by gentle inversions. Ultimately, centrifugation was performed at 10000 x *g* for 1.5 min at RT. Supernatants were collected into DEPC treated microcentrifuge tubes. To check contaminants in the samples, samples were analyzed at nanodrop, if there was still some contaminants Zymo RNA Clean and Concentrator Kit (Zymo Research, USA) was used.

RNA concentrations, A_{260}/A_{280} and A_{260}/A_{230} ratios after DNase treatment and cleanup protocol were represented in Appendix Table E.1 and E.2.

2.1.9 Agarose Gel Electrophoresis

After total RNA isolation step, visualization of RNA samples was required to prove that samples do not include any contaminants and having acceptable stability and integrity. Thus, both DNase, cleanup treated and untreated RNA samples were run on 1% agarose gel (Sigma Aldrich, Germany) at 80V for 50 min. For RNA fragment sizing comparison RiboRuler High Range RNA Ladder (Thermo Scientific, USA) was loaded and 2 µl of the samples were mixed with 2 µl 2X loading dye. At the end of the run, visualization was performed under ultraviolet (UV) exposure (Vilber Lourmat UV Imager, Belgium).

2.1.10 Complementary DNA (cDNA) Synthesis

Single stranded RNA samples were converted to cDNAs' by using Thermo Scientific RevertAid First Strand cDNA Synthesis Kit (USA) in BioRad T100 Thermal Cycler (USA). According to manufacturers´instructions 1 µl random hexamer primer was added to RNA samples in PCR tubes and nuclease free water was added to a final volume of 12 µl. Incubation was performed at 65^0C for 5 min. Then, 4 µl 5X reaction buffer, 1 µl Ribolock RNase inhibitor (20 U/µl), 2 µl 10 mM dNTP and finally 1 µl RevertAid M-MuLV reverse transcriptase (200 U/µL) were added as in indicated order. As a negative control, no reverse transcriptase (no RT) samples were used. Incubation was applied at 25^0C for 5 min and then, at 42^0C for 60 min and terminated by heating at 70^0C for 5 min. Newly synthesized cDNA samples were stored at -20^0C until use.

2.1.11 Quantitative Real Time Polymerase Chain Reaction (qRT-PCR)

qRT-PCR is one of the most commonly used sensitive technique for detecting very low amounts of mRNA levels and quantifying changes in terms of gene expression levels (Pfaffl *et al*., 2001). In this method the amount of amplicon is proportional to fluorescence intensity produced by using a widely used fluorescent DNA binding dye named SYBR Green. The first detected target amplification is generally referred as threshold cycle (C_t) is the time point of fluorescence intensity is more than fluorescence of background. qRT-PCR measures the fluorescence at each cycle as the amplification progresses (Marisa *et al*., 2005). Briefly, the more the quantity of starting target DNA in material, the faster a significant fluorescent signal increase will be present, resulting in a lower Ct value (Heid *et al*., 1996). Since the melt curve analysis is also a significant indicator of determining the quality of products, melt curves were also examined at the end of each reaction. Melt curves are basically interpretations of double-stranded DNA denaturation characteristics in the course of heating. Melting temperatures (Tm) were shown as the peaks which are referred as the temperature at half of the DNA is denatured (Appendix C). Consequently, melt curves are crucial for understanding amplicons' quality and purity (Ririe *et al*., 1997).

Table 2-1 Primer pairs used in qRT-PCR experiments (FP: forward primer, RP: reverse primer).

Primer ID and NCBI accession number	Oligonucleotide Sequence	Amplicon Size
GAPDH (NM_017008)	FP: 5' – TCCCATTCTTCCACCTTT – 3'	92 bp
	RP: 5' – TAGCCATATTCATTGTCATACC – 3'	
POMC (NM_139326)	FP: 5' – AACATCTTCGTCCTCAGA – 3'	80 bp
	RP: 5' – CGACTGTAGCAGAATCTC – 3'	
NPY (NM_012614)	FP: 5' – AATGAGAGAAAGCACAGAAA – 3'	89 bp
	RP: 5' – AAGTCAGGAGAGCAAGTT – 3'	

Table 2-2 Optimized qRT-PCR mixtures of *GAPDH*.

Reaction Components	Volume
SybrGreen Mix	10 µl
Forward primer (5 µM)	1.6 µl
Reverse primer (5 µM)	1.6 µl
cDNA	4 µl
$MgCl_2$ (25mM)	2.4 µl
Nuclease free water	0.4 µl
Total volume	20 µl

Table 2-3 Reaction conditions of *GAPDH*.

	Temperature	**Time**	**Cycle**
Initial denaturation	94^0C	15 min	35
Denaturation	94^0C	20 sec	
Annealing	57^0C	30 sec	
Extention	72^0C	30 sec	
Melt	50^0C - 99^0C		

Table 2-4 Optimized qRT-PCR mixtures of *NPY*.

Reaction Components	**Volume**
SybrGreen Mix	10 µl
Forward primer (5 µM)	0.4 µl
Reverse primer (5 µM)	0.4 µl
cDNA	4 µl
$MgCl_2$ (25mM)	2.4 µl
Nuclease free water	2.8 µl
Total volume	20 µl

Table 2-5 Reaction conditions of *NPY*.

	Temperature	**Time**	**Cycle**
Initial denaturation	94^0C	15 min	50
Denaturation	94^0C	20 sec	
Annealing	53^0C	15 sec	
Extention	72^0C	20 sec	
Melt	50^0C - 99^0C		

Table 2-6 Optimized qRT-PCR mixtures of *POMC*.

Reaction Components	**Volume**
SybrGreen Mix	10 µl
Forward primer (5 µM)	0.8 µl
Reverse primer (5 µM)	0.4 µl
cDNA	4 µl
$MgCl_2$ (25mM)	2.4 µl
Nuclease free water	2.4 µl
Total volume	20 µl

Table 2-7 Reaction conditions of *POMC*.

	Temperature	Time	Cycle
Initial denaturation	94^0C	15 min	45
Denaturation	94^0C	20 sec	
Annealing	63^0C	30 sec	
Extention	72^0C	20 sec	
Melt	50^0C - 99^0C		

Threshold cycles (C_t) of each group were recorded and used for the calculation of fold changes in terms of candidate genes' expression levels. Since the reaction efficiencies of genes were not substantially different from each other, the $2^{-\Delta\Delta C}{}_T$ method (Livak *et al*., 2001) was used. The calculation formula was depicted below:

$$\Delta Ct = Ct\ (target) - Ct\ (reference)$$

$$\Delta\Delta Ct = \Delta Ct\ (treatment) - \Delta Ct\ (control)$$

$$Fold\ difference = 2^{-\Delta\Delta C}{}_T$$

2.2 STATISTICAL ANALYSIS

Statistical analyses of all experiments were performed by using GraphPad Prism 6 (GraphPad Software Inc., USA). For group analysis, one way analysis of variance (ANOVA) and for individual analysis, unpaired t-test were applied. Data were calculated and represented as mean ± standard error mean (SEM).

CHAPTER 3

RESULTS AND DISCUSSION

3.1 RAT STUDIES

3.1.1 Weight Changes and Food Consumption

Rats were weighed weekly to determine the effect of different amount of food consumptions on the body weight from beginning to the end of the experiment. No significant change was observed between groups according to the mean group weights of animals (Fig. 3.1).

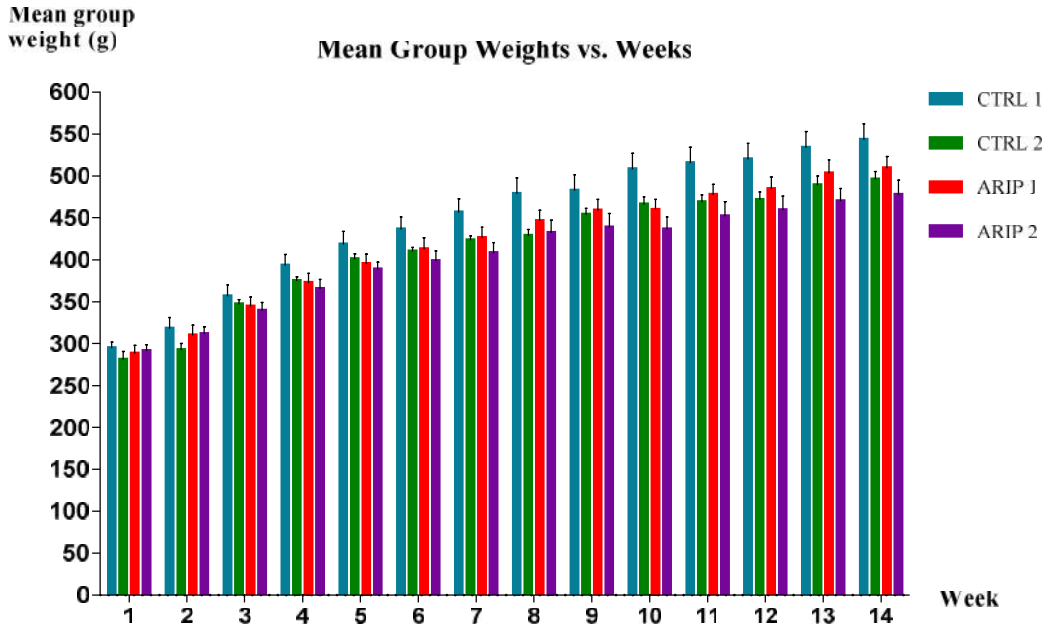

Figure 3-1 Mean rat weights according to weeks. The values are depicted as Mean ± SEM.

After the 14 week period of food consumption the results of mean weight calculation signified that only sucrose administered control group (CTRL 1) gained 248.80 ± 11.83 g whereas metformin administered second control group (CTRL 2) gained 215.20 ± 0.65 g. On the other hand aripiprazole administered (ARIP 1) group gained 221.0 ± 4.55 g and 7 week metformin, 7 week aripiprazole administered (ARIP 2) group gained 186.29 ± 10.24 g (Fig 3.2). These calculations demonstrated that ARIP 2 group trended to gain less weight compared with the rest of the groups; however, no statistically significant difference was observed between the groups.

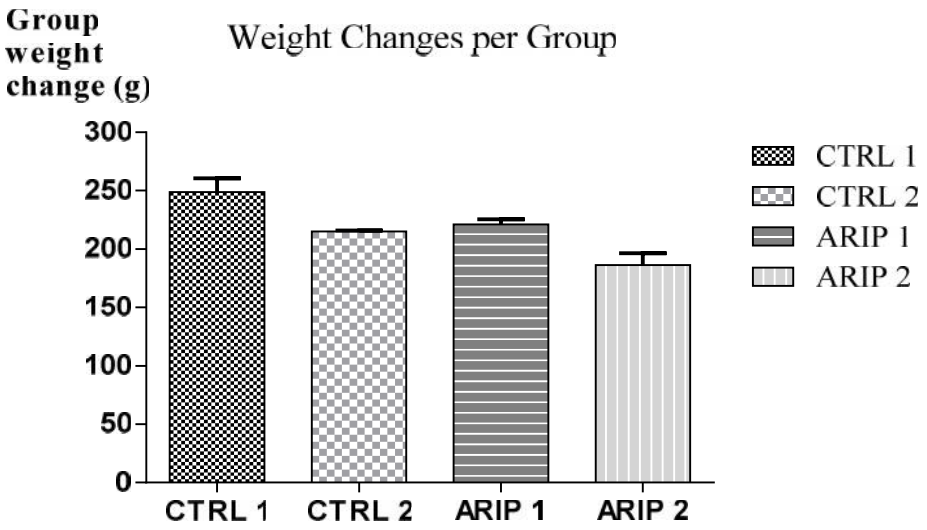

Figure 3-2 Weight changes of groups after 14 weeks. The values are depicted as Mean ± SEM.

Average meal size consumption values were calculated for each group and trend line measurements indicated that CTRL 1 group had more food consumption with respect to other groups (Fig. 3.3). Metformin and aripiprazole co-administered group had the least amount of food consumption with having a statistically significant deviation ($p<0.01$). According to the ARIP 2 group's descending trend line, the food intake inhibition by metformin might be more pronounced in the aripiprazole treatment compared to 14 weeks metformin administered treatment implying that metformin and aripiprazole caused an apparent decrease in terms of appetite.

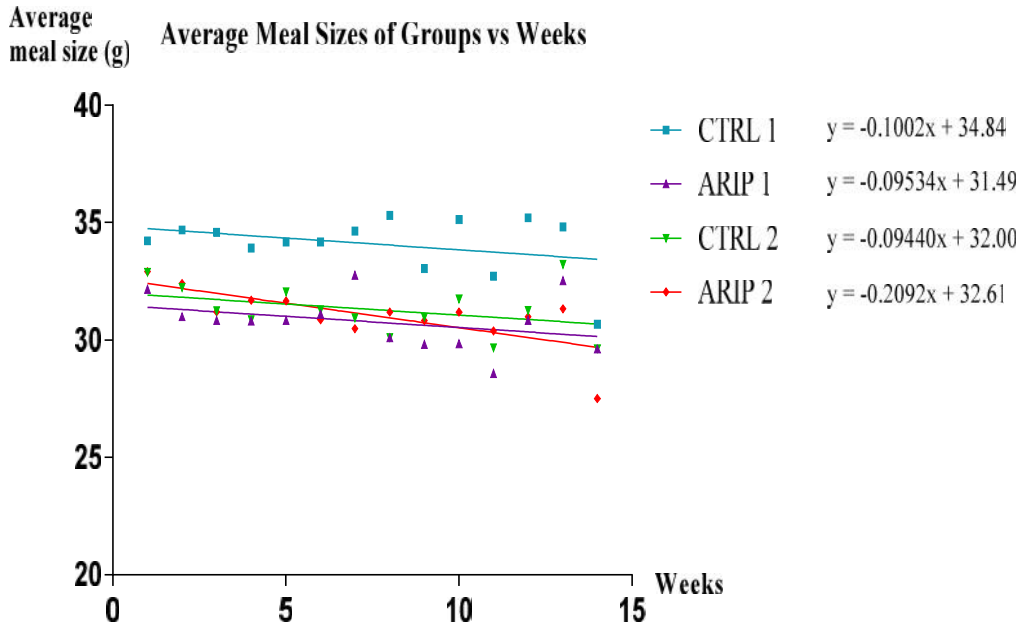

Figure 3-3 Average meal sizes of groups according to weeks.

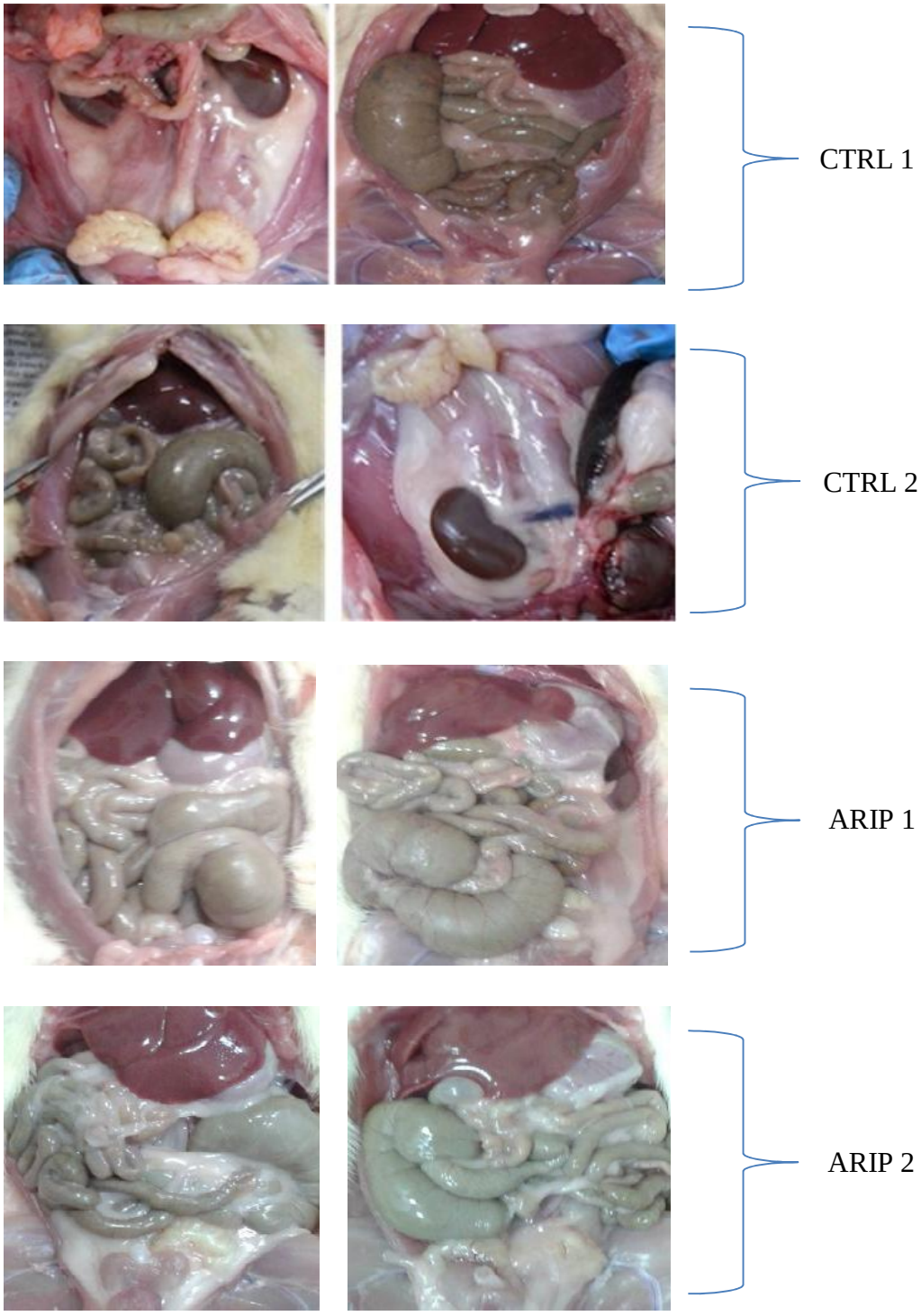

Figure 3-4 Abdominal adiposity images of rats.

3.1.2 Triglyceride Concentrations

Since there is a substantial correlation between plasma triglyceride levels and obesity, triglyceride concentrations of the rats were measured. The aim of this experiment was to determine the effects of metformin and aripiprazole treatments on lipid profile. Results of the triglyceride levels indicated that there was no statistically significant change between animal groups (Fig. 3.5). After the 14 weeks period of food consumption, animal groups' mean triglyceride concentrations were 0.99 $\pm$ 0.11 mM for CTRL 1, 1.39 $\pm$ 0.08 mM for CTRL 2, 1.22 $\pm$ 0.12 mM for ARIP 1 and 1.11 $\pm$ 0.14 mM for ARIP 2 respectively.

According to the human studies, metformin was known to decrease plasma triglyceride levels (Wulffele *et al*., 2004) however, some contrary results were observed in different studies as well. For instance, no statistically significant triglyceride level change was detected after 10 weeks of metformin treatment in humans (Ranganathan *et al*., 2006).

In this study, lower plasma triglyceride levels were expected in the control group and in metformin treated rats but no significant changes were observed. It might be due to intragroup variations of the animals. Also the genetic heterogeneity of the animals could be another contributing factor. Since our animals were outbred animals, this factor should be taken into consideration as well.

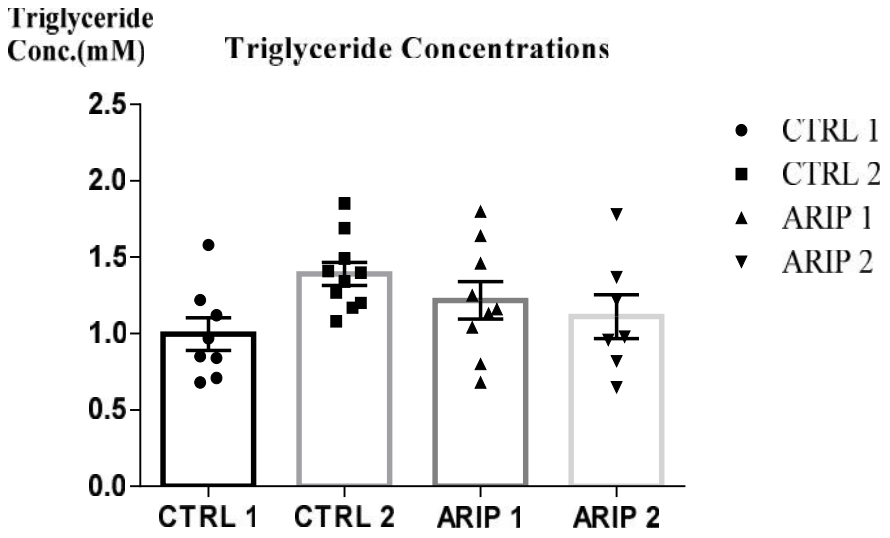

Figure 3-5 Triglyceride concentrations of rat groups. The values are depicted as Mean ± SEM.

According to the Adult Treatment Panel III report, weight loss elevates hypertriglyceridemia in a notable manner (Adult Treatment Panel III, 2002). Similarly our experimental results demonstrate that metformin and aripiprazole lead to a reasonable amount of appetite loss and slightly increased amount of triglyceride levels.

3.1.3 Leptin Concentrations

Plasma leptin concentrations were calculated to observe adiposity level changes in the case of metformin and aripiprazole administrations. According to the unpaired t-test analysis results, statistically significant differences between CTRL 1 group 2.03 $\pm$ 0.07 ng/ml vs ARIP 1 group 3.40 $\pm$ 0.10 ng/ml and between CTRL 2 group 1.49 $\pm$ 0.04 ng/ml vs ARIP 2 group 2.68 $\pm$ 0.09 ng/ml plasma leptin were found (Fig. 3.6). Metformin administration slightly reduced leptin levels which is also correlated with some of the recent studies. Leptin levels were found to be decreased in metformin received high fat fed rats (Kim *et al*., 2006). Additionally in human studies, metformin treatment caused significant reduction in terms of plasma leptin concentrations (Kadhim *et al*., 2012). Also, there were some findings that observed no significant change in terms of leptin levels (Adamia *et al*., 2007). Different results in literature might be because of the variations in animal types, drug amounts or duration time.

Since aripiprazole is one the weight neutral antipsychotics, studies in the literature have not focused on relationship between weight gain and leptin so far. To our knowledge, this study provides the first evidence of aripiprazole effects on body weight and leptin levels in Wistar rats. Interestingly, elevated plasma leptin levels were detected in aripiprazole groups with respect to the controls which was correlated with a study that was conducted in humans. In female patients treated with aripiprazole but not with ziprasidone leptin levels were increased (Pérez-Iglesias *et al*., 2014).

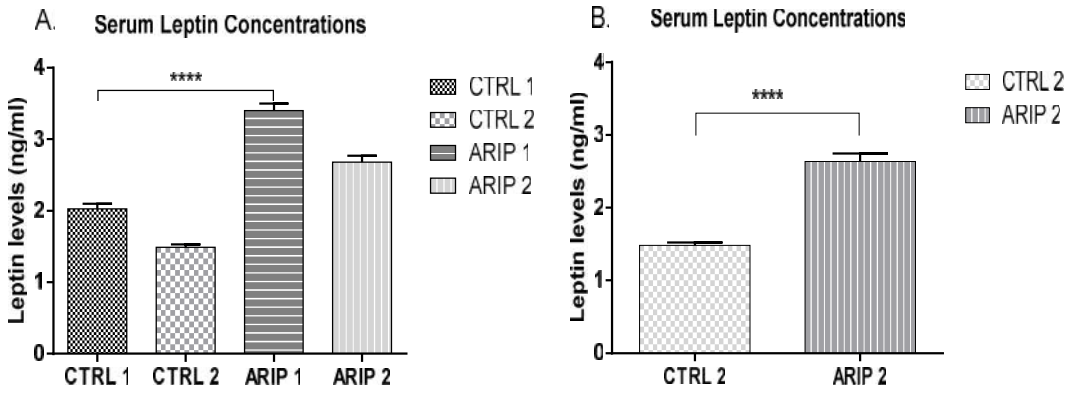

Figure 3-6 Leptin concentrations of rat groups. A. Analysis results of unpaired t-test applied to CTRL 1 and ARIP 1 groups. B. Analysis results of unpaired t-test applied to CTRL 2 and ARIP 2 groups. **** $p<0.0001$. The values are depicted as Mean $\pm$ SEM.

3.1.4 RNA Concentrations and Agarose Gel Electrophoresis

Hypothalamic RNA concentrations, A_{260}/A_{280} and A_{260}/A_{230} ratios were calculated. A ratio of ~1.8 is generally accepted as "pure" for DNA; on the other hand, a ratio of ~2.0 indicates RNA purity (Pfaffl, 2006).

Total RNA samples were run on 1% agarose gel in order to confirm their purity and integrity. Agarose gel images demonstrated that total RNA was intact and free of DNA contamination after DNase treatment. Also 3 ribosomal RNA bands (28S, 18S and 5S) were observed. These rRNA bands represent the integrity of eukaryotic RNA's (Figure F.1 - F.4 in Appendix F).

3.1.5 qRT-PCR Results of Candidate Genes in Rat Hypothalamus

Absolute quantification and relative quantification methods are prevalently used methods in order to analyze quantitative real-time PCR (qRT-PCR) data. Absolute quantification detects the input copy number, generally by relating the PCR signal to a standard curve. On the other hand relative quantification relates the PCR signal of the target transcript in a treatment group to that of another sample such as an untreated control. The $2^{-\Delta\Delta C_T}$ (Livak) method is an appropriate way to analyze the relative changes in gene expression from qRT-PCR experiments (Livak and Schmittgen, 2001).

Relative quantification is based on normalizing the expression of a target gene to the expression of a reference gene, which serves as an internal standard, and on comparing the expression of these normalized gene expressions in target versus control samples (calibrators). To obtain accurate results with this type of quantification, it is necessary to include one or more stable internal standards (housekeeping genes), that are not expected to change their expressions under selected experimental conditions (Livak and Schmittgen, 2001; Pfaffl *et al.*, 2004; Valasek and Repa, 2005; Yuan *et al.*, 2006).

3.1.5.1 Standard Curves of Candidate Genes

Standard curves were constructed for *GAPDH, POMC* and *NPY* in order to calculate mRNA expression levels in the rat hypothalamic tissues. Standard curves, melt curves and agarose gel images of qRT-PCR were depicted in Appendix B.

3.1.5.2 Fold Changes of Candidate Gene Expression Levels

The fold changes of the candidate gene expressions were calculated and represented in Fig. 3.7 and Fig. 3.8 as bar graphs. All of the Ct values were respresented in Appendix C.

NPY expression levels were significantly lower in metformin and aripiprazole administered groups which was an expected outcome. On the other hand, *POMC* expressions were also observed as significantly down regulated which was an interesting result. Because *POMC* is an anorexigenic, and *NPY* is an orexigenic neuropeptide they should have act as antagonistically. There might be still some poorly understood machanisms related to *POMC* actions.

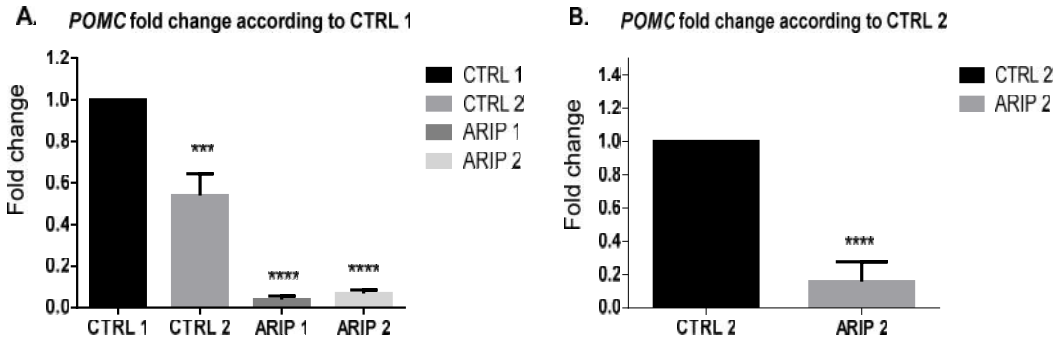

Figure 3-7 Fold changes of *POMC* expression levels in all groups. A. Analysis results of one-way ANOVA applied to all groups. B. Analysis results of unpaired t-test applied to CTRL 2 and ARIP groups. *** $p<0.001$, **** $p<0.0001$. The values are depicted as Mean $\pm$ SEM.

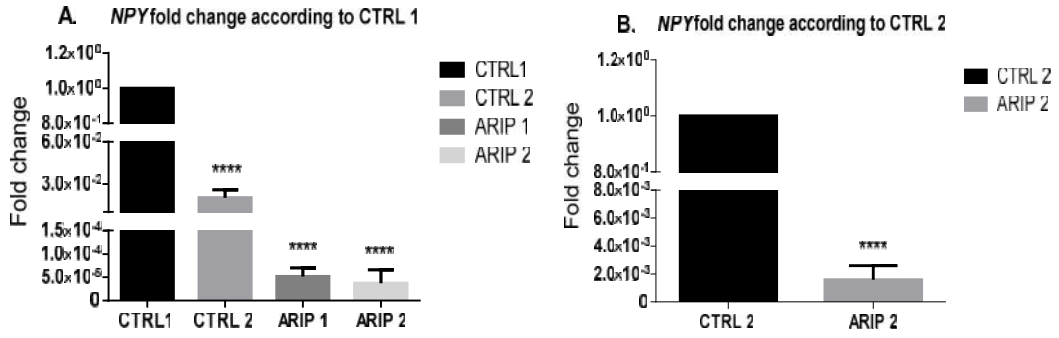

Figure 3-8 Fold changes of *NPY* expression levels in all groups. A. Analysis results of one-way ANOVA applied to all groups. B. Analysis results of unpaired t-test applied to CTRL 2 and ARIP groups. **** $p<0.0001$. The values are depicted as Mean $\pm$ SEM.

Briefly, the results of this study demonstrated that there were not significant changes in terms of weight gain and triglyceride levels between groups under metformin and aripiprazole administration however; we found out significant changes in terms of *NPY* and *POMC* mRNA levels. With that valuable data, we are now trying to optimize western blot studies in order to confirm these differences by showing alteration of *NPY* and *POMC* protein levels.

There are also other studies conducted with adolescents and children. Metformin treatment in 15 patients from total of 19 resulted in significant weight loss (Morrison *et al*., 2002). It has also been suggested that metformin might decrease production of hepatic glucose through the increased phosphorylation and AMPK pathway activation which resulted in the suppression of acetyl-CoA carboxylase (ACC) activity in hepatocytes (Zhou *et al*., 2001). According to another study, it was also demonstrated that after 4 weeks of oral metformin administration, *NPY* expression

levels in the hypothalami were significantly dropped whereas *POMC* expression levels remained the same (Lv *et al*., 2012).

It is evident that there is inconsistency in the literature between the reported data about the effect of metformin on hypothalamic weight control mechanisms. Also, there is still a lack of information in the literature about the long-term effects of metformin administration on hypothalamic mechanisms.

Evidenced that aripiprazole might have some effects of protection against weight gain which may be related to the partial agonistic effect on 5-HT1A receptors (Reynolds *et al*., 2006; Kirk *et al*., 2004). Moreover aripiprazole might also involve partial agonism on dopamine D2 and some forms of the partial agonism on 5-HT2C receptor (Zhang *et al*., 2006).

Standard chow diet was the only available food choice which was a closely related factor in terms of weight and appetite increase. Additionally, the used number of animals may be increased to reach statistically correct results such as weight gain. Apart from these, intra group variations were observed similar to other studies; yet, most of these limitations may probably be overcome upon increasing the animal numbers.

CHAPTER 4

CONCLUSION

- This study demonstrated metformin and aripiprazole effect on the appetite mechanism and food intake.

- Weight gains and plasma triglyceride were observed to be unaffected by both metformin and aripiprazole treatments. On the other hand, leptin levels were slightly decreased in metformin administered rats whereas significantly increased in aripiprazole administered rats. Additionally, *POMC* and *NPY* expression levels were significantly decreased in metformin and aripiprazole administered rats with respect to sucrose administered control group.

- Additional future studies are required clarify whether there are any other playing factors in aripiprazole and the *POMC* action. Also, the hypothalamic protein levels of the candidate genes will be further studied.

REFERENCES

Adamia N., Virsaladze D., Charkviani N., Skhirtladze M., Khutsishvili M. (2007) "Effect of metformin therapy on plasma adiponectin and leptin levels in obese and insulin resistant postmenopausal females with type 2 diabetes", *Georgian Medical News*, 52-55.

Allison D.B., Kaprio J., Korkeila M., Koskenvuo M., Neale M.C., Hayakawa K. (1996) "The heritability of body mass index among an international sample of monozygotic twins reared apart", *Int J Obes Relat Metab Disord.*, 20: 501–506.

Alvarez-Jime´nez M., Gonza´lez-Blanch C., Va´zquezBarquero J.L., *et al*. (2006) "Attenuation of antipsychotic induced weight gain with early behavioral intervention in drug-naive first-episode psychosis patients: a randomized controlled trial", *J Clin Psychiatry*., 67(8): 1253-1260.

Andreasen C.H., Stender-Petersen K.L., Mogensen M.S., Torekov S.S., Wegner L., Andersen G., *et al*. (2008) "Low physical activity accentuates the effect of the FTO rs9939609 polymorphism on body fat accumulation", *Diabetes*, 57, 95–101.

Aponte Y., Atasoy D., Sternson S.M. (2011) "AGRP neurons are sufficient to orchestrate feeding behavior rapidly and without training", *Nature Neuroscience*, 14: 351–355.

Atasoy, D. *et al*. (2012) "Deconstruction of a neural circuit for hunger", *Nature* 488, 172–177.

Atkinson R.L. (2005) "Etiologies of obesity", *The Management of Eating Disorders and Obesity Nutrition and Health* , pp 105-118.

Baptista T., Martınez J., Lacruz A., *et al*. (2006) "Metformin for prevention of weight gain and insulin resistance with olanzapine: a double-blind placebocontrolled trial", *Can J Psychiatry*. 51(3): 192-196.

Bates S.H., Stearns W.H., Dundon T.A., Schubert M., Tso A.W., Wang Y., Banks A.S., Lavery H.J., Haq A.K., Maratos-Flier E., *et al*. (2003) "STAT 3 signalling is required for leptin regulation of energy balance but not reproduction", *Nature* 421, 856–859.

Block L., Schemling L., Couto A., Mourao S., & Bresolin T. (2008) "Pharmaceutical equivalance of metformin tablets with various binders", *Journal of Basic and Applied Pharmaceutical Sciences*, 29-35.

Campfield L.A., Smith F.J., Guisez Y., Devos R., Burn P. (1995) "Recombinant mouse OB protein: evidence for a peripheral signal linking adiposity and central neural networks", *Science* 269, 546–549.

Ceddia R.B., William N.B., Curi R., (2001) "The response of skeletal muscle to leptin", *Frontiers in Bioscience* 6.

Chambers A.P. Jessen L, Ryan K.K., *et al*. (2011) "Weight-independent changes in blood glucose homeostasis after gastric bypass or vertical sleeve gastrectomy in rats", *Gastroenterology*, 141: 950-958.

Chagnon Y.C, Rankinen T, Snyder E.E, Weisnagel S.J, Perusse L, Bouchard C. (2003) "The human obesity gene map: the 2002 update", *Obes Res*, 11: 313–367.

Chue P. (2004) "The assessment and management of antipsychotic-associated metabolic disturbances from a psychiatric perspective", *Can J Psychiatry*, 49(3): 200-207.

Clark J.T., Kalra P.S., Crowley W.R., Kalra S.P. (1984) "Neuropeptide Y and human pancreatic polypeptide stimulate feeding behavior in rats", *Endocrinology*, 115, 427–429.

Cone R.D. (2006) "Studies on the physiological functions of the melanocortin system", *Endocr Rev*., 27(7), 736-49.

Cooper S.J. and Al-Naser H.A. (2006) "Dopaminergic control of food choice: contrasting effects of SKF 38393 and quinpirole on highpalatability food preference in the rat", *Neuropharmacology*, 50, 953–963.

Dores R.M. & Lecaude S. (2005) "Trends in the evolution of the proopiomelanocortin gene", *General and Comparative Endocrinology*, 142 81–93.

Eknoyan, Garabed (2007) "Adolphe Quetelet (1796–1874)—the average man and indices of obesity", *Nephrology Dialysis Transplantation* 23 (1): 47–51.

Farooqi I.S., Keogh J.M., Yeo G.S., Lank E.J., Cheetham T., O'Rahilly S. (2003) "Clinical spectrum of obesity and mutations in the melanocortin 4 receptor gene", *N Engl J Med*., 348: 1085e95.

Folsom A.R., Kushi L.H., Anderson K.E., Mink P.J., Olson J.E. and Hong C.P., *et al*. (2000) "Association of general and abdominal obesity with multiple health outcomes in older women", *Arch Intern Med*., 160: 2117-28.

Frayling T.M., Timpson N.J., Weedon M.N., Zeggini E., Freathy R.M., Lindgren C.M., *et al*. (2007) "A common variant in the FTO gene is associated with body mass index and predisposes to childhood and adult obesity", *Science* 316, 889–894.

Friedman J.M., Halaas J.L., (1998) "Leptin and the regulation of body weight in mammals", *Nature* 395, 763–770.

Fujii N., Jessen N. & Goodyear L.J. (2006) "AMP-activated protein kinase and the regulation of glucose transport", *American Journal of Physiology*. Endocrinology and Metabolism 291 E867–E877.

Funahashi H., Hori T., Shimoda Y., Mizushima H., Ryushi T., Katoh S., Shioda S. (2000) "Morphological evidence for neural interactions between leptin and orexin in the hypothalamus", *Regulat. Pept*. 92 (1–3), 31–35.

Gantz I. & Fong T.M. (2003) "The melanocortin system", *Am. J Physiol Endocrinol Metab*., 284(3): E468-74.

Gehlert D.R. (2004) "Introduction to the reviews on Neuropeptide Y", *Neuropeptides* 38 (4), 135–140.

Gropp E., Shanabrough M., Borok E., Xu A.W., Janoschek R., Buch T., Plum L., Balthasar N., Hampel B., Waisman A., Barsh G.S., Horvath T.L., Bruning J.C. (2005) "Agouti-related peptide-expressing neurons are mandatory for feeding", *Nature Neuroscience*, 8: 1289 –1291.

Halford, J.C.G. *et al*. (2011) "Serotonergic anti-obesity agents: past experience and future prospects", *Drugs* 71, 2247–2255.

Haupt A., Thamer C., Machann J., Kirchhoff K., Stefan N., Tschritter O., *et al*. (2008) "Impact of variation in the FTO gene on whole body fat distribution, ectopic fat, and weight loss", *Obesity* (Silver Spring) 16, 1969–1972.

Heid C.A., Stevens J., Livak K.J., and Williams P.M. (1996) "Real time quantitative PCR", *Genome Res*., 6: 986-994.

Ho S.C., Chen Y.M., Woo J.L., Leung S.S., Lam T.H., Janus E.D. (2001) "Association between simple anthropometric indices and cardiovascular risk factors", *Int Obes Relat Metab Disord*, 25: 1689-97.

Inui A. (2000) "Transgenic approach to the study of body weight regulation", *Pharmacol. Rev*., 52 (1), 35–62.

Kadhim K., Ismael D., Khalaf B., Hussein K., Zalzala M., & Hussain S. (2012) "Dose-dependent relationship between serum metformin levels and glycemic control, insulin resistance and leptin levels in females newly diagnosed with type 2 diabetes mellitus", *Journal of Diabetes Mellitus*, 179-185.

Kalra S.P., Dube M.G., Sahu A., Phelps C., Kalra P.S. (1991) "Neuropeptide Y secretion increases in the paraventricular nucleus in association with increased appetite for food", *Proc. Natl. Acad. Sci*. USA 38, 10931–10935.

Kim Y.W., Kim J.Y., Park Y.H., Park S.Y., Won K.C., Choi K.H., *et al*. (2006) "Metformin restores leptin sensitivity in high-fat-fed obese rats with leptin resistance", *Diabetes*, 716-724.

Kirk S., Neill J., Jones D. and Reynolds G. (2004) "Ziprasidone suppresses olanzapine-induced increases in ingestive behaviour in the rat", *Eur J Pharmacol.* 505: 253–254.

Könner A.C., Brüning J.C. (2012) "Selective insulin and leptin resistance in metabolic disorders", *Cell Metab*., 16(2): 144–52.

Kurşungöz C. (2012, August) "Determination of hypothalamic neuropeptide levels involved in appetite regulation in atypical antipsychotic drug, Risperidone treatment", *Master Thesis submitted to Graduate School of Natural and Applied Sciences, METU*. Ankara, Turkey.

Kurt G. (2014, July) "Effects of metformin on olanzapine induced weight gain in male Wistar rats: The change of hypothalamic neurohormones involved in body weight regulation", *Master Thesis submitted to Graduate School of Natural and Applied Sciences, METU*. Ankara, Turkey.

Lam D.D. *et al*. (2007) "Serotonin 5-HT2C Receptor agonist promotes hypophagia via downstream activation of melanocortin 4 receptors", *Endocrinology*, 149, 1323–1328.

Licinio J., Caglayan S., Ozata M., Yildiz B.O., de Miranda P.B., O'Kirwan F., Whitby R., Liang L., Cohen P., Bhasin S., *et al*., (2004) "Phenotypic effects of leptin replacement on morbid obesity, diabetes mellitus, hypogonadism, and behavior in leptin-deficient adults", *PNAS* 101, 4531–4536.

Lee G.H., Proenca Montez J.M., Carroll K.M., Darvishzadeh J.G., Lee J.I., Friedman J.M., (1996) "Abnormal splicing of the leptin receptor in diabetic mice", *Nature* 379, 632–635.

Lee Y.S., Poh L.K., Loke K.Y. (2002) "A novel melanocortin 3 receptor gene (MC3R) mutation associated with severe obesity", *J Clin Endocrinol Metab*, 87: 1423e6.

Lin H.Z., et al. (2000) "Metformin reverses fatty liver disease in obese, leptin-deficient mice", *Nature Medicine*, 6: 998-1003.

Livak K.J., Schmittgen T.D. (2001) "Analysis of relative gene expression data using real-time quantitative PCR and the $2^{-\Delta\Delta Ct}$ method", *Methods*, 25: 402–408.

Lv W.S., Wen J.P., Li L., Sun R.X., Wang J., Xian, Y.X., Cao C.X., Wang Y.L., Gao Y.Y. (2012). "The effect of metformin on food intake and its potential role in hypothalamic regulation in obese diabetic rats", *Brain Research*, 11-19.

Maffei M., Halaas J., Ravussin E., Pratley R.E. Lee G.H., Zhang Y., Fei H., Kim S., Lallone R., Ranganathan S., *et al*. (1995) "Leptin levels in human and rodent: measurement of plasma leptin and ob RNA in obese and weight reduced subjects". *Nature Medicine*, 1, 1155–1161.

Mantzoros C.S., Flier J.S. (2000) "Leptin as a therapeutic agent", Trials and tribulations. *J Clin Endocrinol Metab*., 85: 4000-2.

Marisa L.W. and Juan F.M. (2005) "Real-time PCR for mRNA quantitation", *BioTechniques*, 39: 75-85.

Meister B. (2000) "Control of food intake via leptin receptors in the hypothalamus", *Vitam. Horm*. 59, 265–304.

Morrison J.A., Cottingham E.M., Barton B.A. (2002) "Metformin for weight loss in pediatric patients taking psychotropic drugs", *Am J Psychiatry*. 159(4): 655-657.

Morton G.J., Cummings D.E., Baskin D.G., Barsh G.S., Schwartz M.W. (2006) "Central nervous system control of food intake and body weight", *Nature* 443:289 – 295.

Muennig P., Lubetkin E., Jia H., Franks P. (2006) "Gender and the burden of disease attributable to obesity", *Am J Public Health*, 96(9): 1662–1668.

Newcomer J.W. (2005) "Second-generation (atypical) antipsychotics and metabolic effects: a comprehensive literature review", *CNS Drugs*. 19 (suppl 1): 1-93.

Niswender K.D., Morton G.J., Stearns W.H., Rhodes C.J., Myers M.G., Jr., and Schwartz M.W. (2001) "Intracellular signaling. Key enzyme in leptin induced anorexia", *Nature* 413, 794–795.

Obesity: preventing and managing the global epidemic. Report of a WHO consultation on obesity. June 3–5, 1997. WHO/NUT/NCD/ 98.1, i-xv, 1–276. 1998. Geneva, Switzerland: World Health Organization.

Padilla S.L., Reef D., Zeltser L.M. (2012) "Defining POMC neurons using transgenic reagents: impact of transient POMC expression in diverse immature neuronal populations", *Endocrinology*, 153: 1219 –1231.

Palmiter R.D. (2007) "Is dopamine a physiologically relevant mediator of feeding behavior? "*Trends Neuroscience*, 30, 375–381.Pedrazzini T. (2004) "Importance of NPY Y1 receptor-mediated pathways: assessment using NPY Y1 receptor knockouts", *Neuropeptides* 38 (4), 267–275.

Pérez-Iglesias R., Ortiz-Garcia de la Foz V., Martínez García O., Amado J.A., Garcia-Unzueta M.T., Ayesa-Arriola R., Suarez-Pinilla P., Tabares-Seisdedos R., Crespo-Facorro B. (2014) "Comparison of metabolic effects of aripiprazole, quetiapine and ziprasidone after 12 weeks of treatment in first treated episode of psychosis", *Schizophrenia Research* 159 (1), 90-4.

Pernicova I., Korbonits M. (2014) "Metformin mode of action and clinical implications for diabetes and cancer", *Nature Reviews Endocrinology*, 143-156.

Peyron C., Faraco J., Rogers W., Ripley B., Overeem S., Charnay Y., Nevsimalova S., Aldrich M., Reynolds D., Albin R., Li R., Hungs M., Pedrazzoli M., Padigaru M., Kucherlapati M., Fan J., Maki R., Lammers G.J., Bouras C., Kucherlapati R., Nishino S., Mignot E. (2000) "A mutation in early onset narcolepsy and a generalized absence of hypocretin peptides in human narcoleptic brains", *Nature Medicine*, 6: 991-997.

Pfaffl M.W., Hageleit M. (2001) "Validities of mRNA quantification using recombinant RNA and recombinant DNA external calibration curves in real-time RT–PCR", *Biotechnol. Lett*., 23, 275–282.

Pfaffl M.W., Tichopad A., Prgomet C., Neuvians T.P. (2004) "Determination of stable housekeeping genes, differentially regulated target genes and sample integrity: BestKeeper – Excel-based tool using pair-wise correlations", *Biotechnol. Lett*., 26: 509–515.

Pfaffl M. (2006) "Relative Quantification in *Real-Time PCR*", New York: Taylor & Francis Group (p. 63-82).

Ranganathan G., Unal R., Pokrovskaya I., Yao-Borengasser A., Phanavanh B., Lecka-Czernik B., *et al*. (2006). The lipogenic enzymes DGAT1, FAS, and LPL in adipose tissue: effects of obesity, insulin resistance, and TZD treatment. *Journal of Lipid Research*, 2444-2450.

Rasouli N., Kern P.A., Reece E.A., Elbein S.C. (2007) "Effects of pioglitazone and metformin on beta-cell function in nondiabetic subjects at high risk for type 2 diabetes", *Am J Physiol Endocrinol Metab*. 292(1): E359-E365.

Reynolds G., Hill M. and Kirk S. (2006) "The 5-HT2C receptor and antipsychotic-induced weight gain - mechanisms and genetics", *J Psychopharmacol.* 20: 15–18.

Ririe K.M., Rasmussen R.P., Wittwer C.T. (1997) "Product differentiation by analysis of DNA melting curves during the polymerase chain reaction". *Anal Biochem.* 245 (2): 154–160.

Schleimer S.B., Johnston G.A.R., Henderson J.M. (2005) "Novel oral drug administration in an animal model of neuroleptic therapy", *Journal of Neuroscience Methods*, 146: 159–164.

Sezlev D. (2012, September 3) "Alterations of hypothalamic neuropeptides involved in food intake and appetite in olanzapine monotherapy", *Master Thesis submitted to Graduate School of Natural and Applied Sciences, METU*. Ankara, Turkey.

Sohn, J.W., *et al*. (2011) "Serotonin 2C receptor activates a distinct population of arcuate pro-opiomelanocortin neurons via TRPC channels", *Neuron* 71, 488–497.

Stanley B.G., Kyrkouli S.E., Lampert S., Leibowitz S.F. (1986) "Neuropeptide Y chronically injected into the hypothalamus: a powerful neurochemical inducer of hyperphagia and obesity", *Peptides* 7, 1189–1192.

Trayhurn P., Hoggard N., Rayner D.V. (2001) "White adipose tissue as a secretory and endocrine organ: Leptin and other secreted proteins", In: Klaus, S. (Ed.), Adipose Tissue. *Landes Bioscience,* Austin, TX.

Tong Y., Pelletier G. (1992) "Role of dopamine in the regulation of proopiomelanocortin (POMC) mRNA levels in the arcuate nucleus and pituitary gland of the female rat as studied by in situ hybridization", *Brain Res. Mol. Brain Res*. 15, 27–32.

Vaisse C., Halaas J.L., Horvath C.M., Darnell J.E. Jr., Stoffel M., Friedman J.M. (1996) "Leptin activation of Stat 3 in the hypothalamus of wild-type and *ob/ob* mice but not *db/db* mice", *Nature Genetics*, 14: 95–97.

Valasek M.A., Repa J.J. (2005) "The power of real-time PCR", *Adv. Physol. Educ*., 29: 151–159.

Vastermark A. & Schiöth H.B. (2011) "The early origin of melanocortin receptors, agouti-related peptide, agouti signaling peptide, and melanocortin receptor-accessory proteins, with emphasis on puffer- fishes, elephant shark, lampreys, and amphioxus", *European Journal of Pharmacology*, 660 61–69.

Welborn T.A., Dhaliwal S.S., Bennett S.A. (2003) "Waist-hip ratio is the dominant risk factor predicting cardiovascular death in Australia", *Medical Journal of Australia*, 179: 580-85.

Wilding J.P., Gilbey S.G., Bailey C.J., Batt R.A., Williams G., Ghatei M.A., Bloom S.R. (1993) "Increased neuropeptide-Y mRNA and decreased neurotensin mRNA in the hypothalamus of the ob/ob mouse", *Endocrinology* 132, 1939–1944.

Williams G., Joanne A., Harrold Cutler D.J., (2000) "The hypothalamus and the regulation of energy homeostasis: Lifting the lid on the black box", *Proc. Nutr. Soc*. 59, 385–396.

Williams K.W. and Elmquist, J.K. (2012) "From neuroanatomy to behavior: central integration of peripheral signals regulating feeding behavior", *Nature Neuroscience* 15, 1350–1355.

Wu Q., *et al*. (2012) "Deciphering a neuronal circuit that mediates appetite", *Nature* 483, 594–597.

Wulffele M., Kooy A., De Zeeuw D., Stehouwer C., Gansevoort R. (2004) "The effect of metformin on blood pressure, plasma cholesterol and triglycerides in type 2", *Journal of Internal Medicine*, 1-14.

Xu A.W., Kaelin C.B., Morton G.J., Ogimoto K., Stanhope K., Graham J., Baskin D.G., Havel P., Schwartz M.W., Barsh G.S. (2005) "Effects of hypothalamic neurodegeneration on energy balance", *PLoS Biol* 3: e415.

Yanik T., Sezlev D., & Ak M. (2013, July 6-11). "Change of hypothalamic and peripheral levels of appetite related hypothalamic neurohormones in olanzapine treated male Wistar rats", *The Federation of European Biochemical Societies (FEBS) poster presentation*. St. Petersburg, Russia.

Yeo G.S.H., Heisler L.K. (2012) "Unraveling the brain regulation of appetite: lessons from genetics", *Nature Neuroscience*, 15(10): 1343-9.

Yuan J.S., Reed A., Chen F., Stewart Jr.C.N. (2006) "Statistical analysis of real-time PCR data", *BMC Bioinformatics*, 22, 7: 85.

Zhang Y.Y., Proenca R., Maffei M., Barone M., Leopold L., Friedman J.M. (1994) "Positional cloning of the mouse obese gene and its human homolog", *Nature* 372, 425–432.

Zhou G., Myers R., Li Y., Chen Y., Shen X., Fenyk-Melody J., *et al*. (2001) "Role of AMP-activated protein kinase in mechanism of metformin action", *Journal of Clinical Investigation*, 1167-1174.

APPENDIX A

PREPARATION AND COMPONENTS OF BUFFERS AND SOLUTIONS

10% Sucrose Solution (w/v)

10 g of sucrose (Sigma-Aldrich, Germany) was dissolved in 100 ml dH_2O by the help of the magnetic stirrer. It was used freshly without storage.

1X Phosphate Buffered Saline

Commercially available tablets for preparation of 0.01 M phosphate buffer with 0.0027 M potassium chloride (KCl) and 0.137 M sodium chloride (NaCl) at pH 7.4 was purchased from Sigma-Aldrich (Germany). According to manufacturer's instructions, 1 tablet was dissolved in 200 ml DEPC-treated water and filtered into DEPC-treated glass bottle and stored at +4^{o}C.

50X Tris-Acetate EDTA (TAE) Buffer, pH 8.0

Table A-1 Prescription for 50X TAE Buffer

Ingredient	**Amount**
Trizma Base (Sigma-Aldrich, Germany)	121 g
Glacial Acetic Acid	28.55 ml
Ethylenediaminetetraacetic acid (EDTA)	37.2 g
Final Volume	500 ml

The indicated amount of Trizma base and EDTA were weighted and about 400 ml dH_2O was added onto them. After that, glacial acetic acid was added and all the components were mixed until fully dissolved by the help of magnetic stirrer. Then pH was adjusted with 2M NaOH (Applichem, Germany) and the volume was added up to 500 ml by dH_2O. After that, the solution was filtered into sterile glass bottle and stored at +4^{o}C. 1X TAE was prepared by 50 fold dilutions from the 50X stock buffer by dH_2O.

1% Agarose Gel Preparation

0.5 g agarose (Sigma-Aldrich, Germany) was weighted and dissolved in 50 ml 1X TAE buffer by heating in the microwave about 2 min (until it was fully dissolved). Then, waited to cool a little bit and 1.5 µl ethidium bromide (EtBr) (Sigma-Aldrich,

Germany) from 10 mg/mL stock solution was added. It was mixed immediately and poured to the electrophoresis gel tank (EasyCast OWL mini - Thermo Scientific, USA). The appropriate combs were placed and left to jellify. After that, 2 µl 1:1 diluted RNA samples were mixed with 2 µl 2X RNA loading dye and loaded into the wells. RNA ladder was loaded into 1 well and the samples were run at 80V for 50 min.

3% Agarose Gel Preparation

It was prepared similar to 1% Agarose gel with only difference in agarose amount (1.5 g agarose /50 ml).

RevertAid First Strand cDNA Synthesis Kit - 5X Reaction Buffer (Thermo Scientific , USA)

- 250 mM Tris-HCl, pH 8.3
- 250 mM KCl
- 20 mM $MgCl_2$
- 50 mM Dithiothreitol (DTT)

SYBR Green JumpStart *Taq* ReadyMix without $MgCl_2$ (Sigma-Aldrich, Germany)

- 20 mM Tris-HCl, pH 8.3
- 100 mM Potassium Chloride (KCl)
- 0.4 mM deoxyadenosine triphosphate (dATP)
- 0.4 mM deoxythymidine triphosphate (dTTP)
- 0.4 mM deoxycytidine triphosphate (dCTP)
- 0.4 mM deoxyguanosine triphosphate (dGTP)
- SYBR Green I dye
- JumpStart *Taq* Antibody
- 0.05 u/µl *Taq* DNA Polymerase
- Glass passivator

APPENDIX B

STANDARD CURVES OF TRIGLYCERIDE

Table B-1 Concentrations of triglyceride standards.

Triglyceride standards	Concentration (mM or µmol/ml)
standard 0	0.00
standard 1	0.04
standard 2	0.08
standard 3	0.12
standard 4	0.16
standard 5	0.20

Table B-2 Concentrations of leptin standards.

Leptin standards	Concentration (pg/ml)
standard 0	2000
standard 1	1000
standard 2	500
standard 3	250
standard 4	125

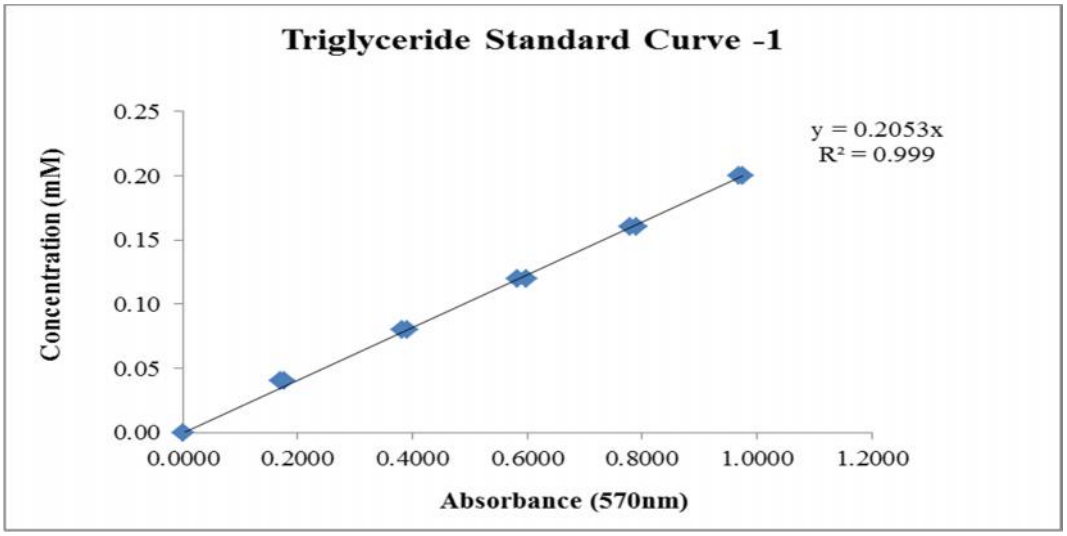

Figure B-1 Triglyceride standard curve 1

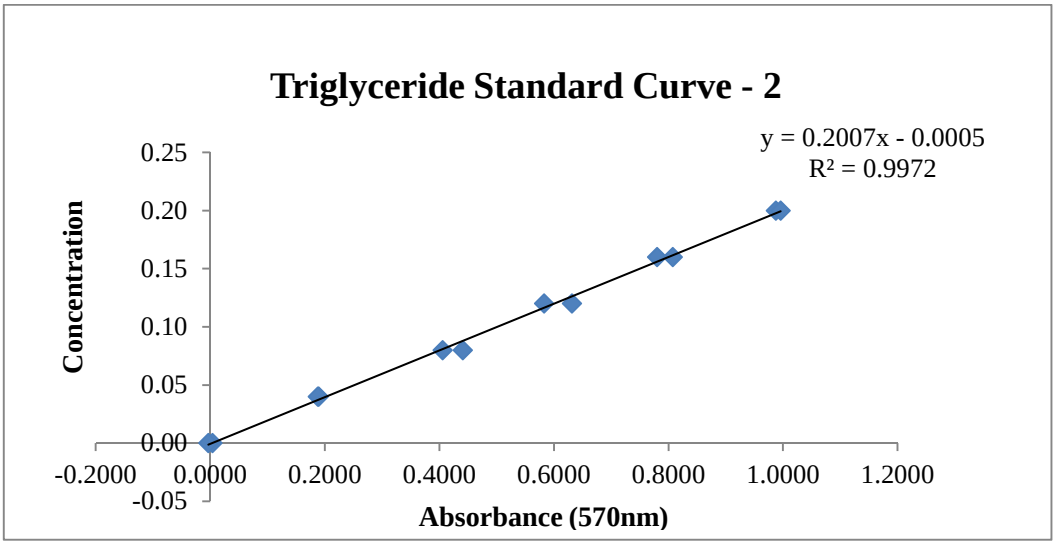

Figure B-2 Triglyceride standard curve 2

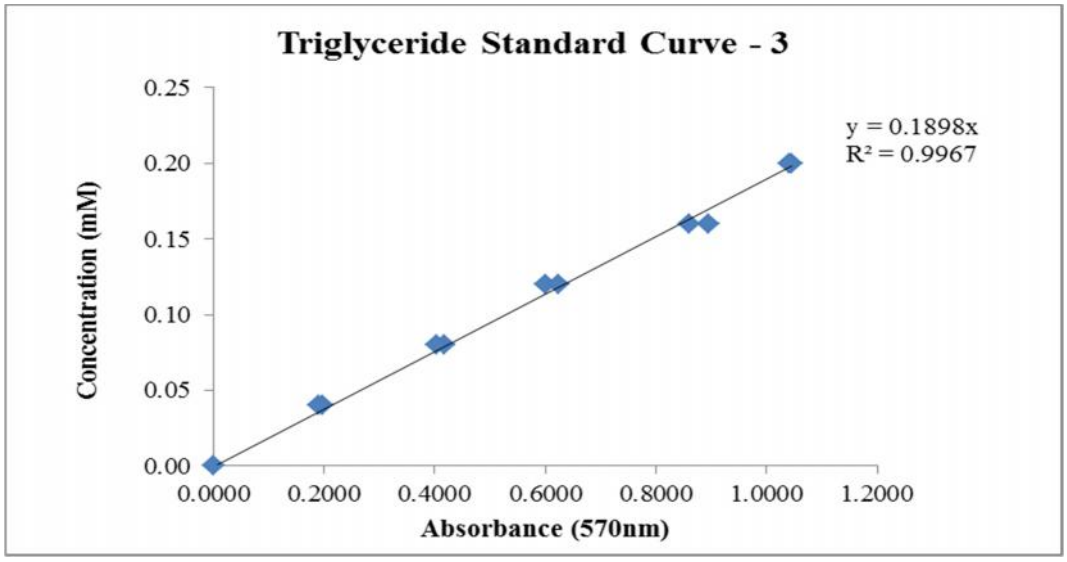

Figure B-3 Triglyceride standard curve 3

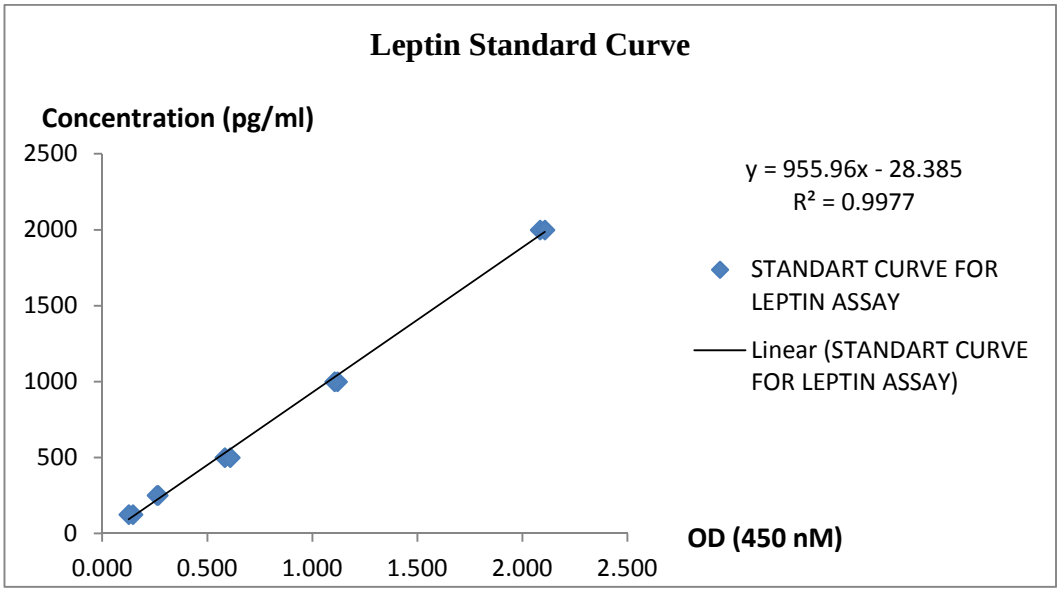

Figure B-4 Leptin standart curve

APPENDIX C

STANDARD CURVES, MELT CURVES AND GEL IMAGES OF qRT-PCR

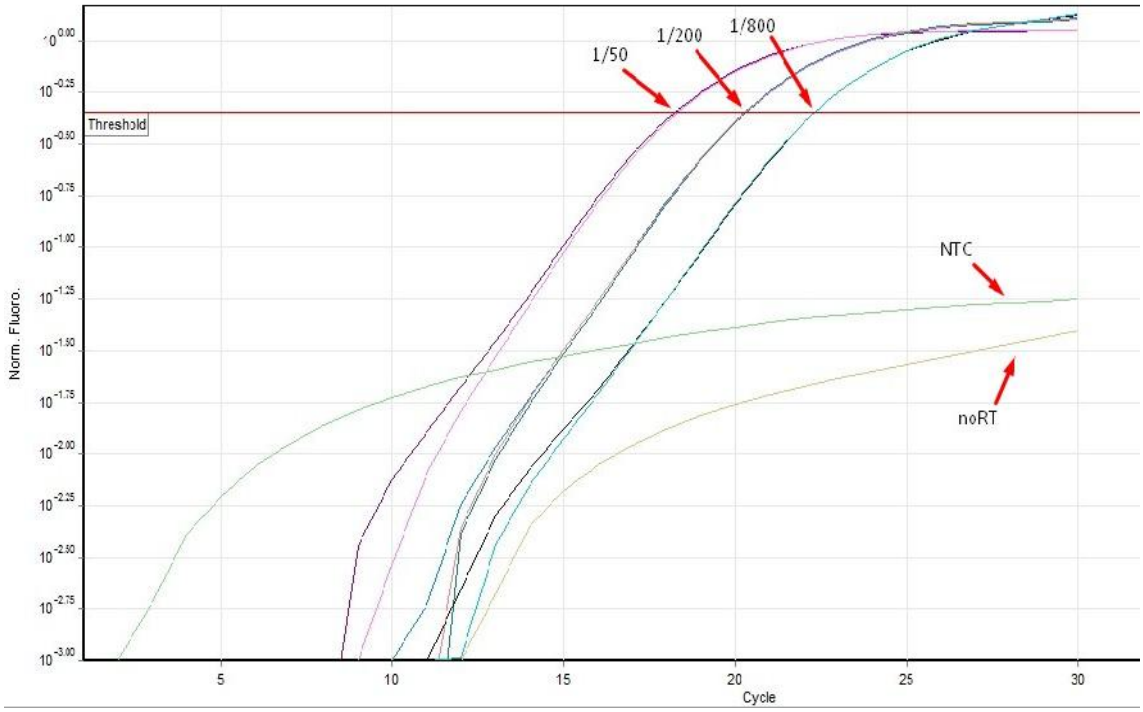

Figure C-1 *GAPDH* standard curve amplification data analysis.

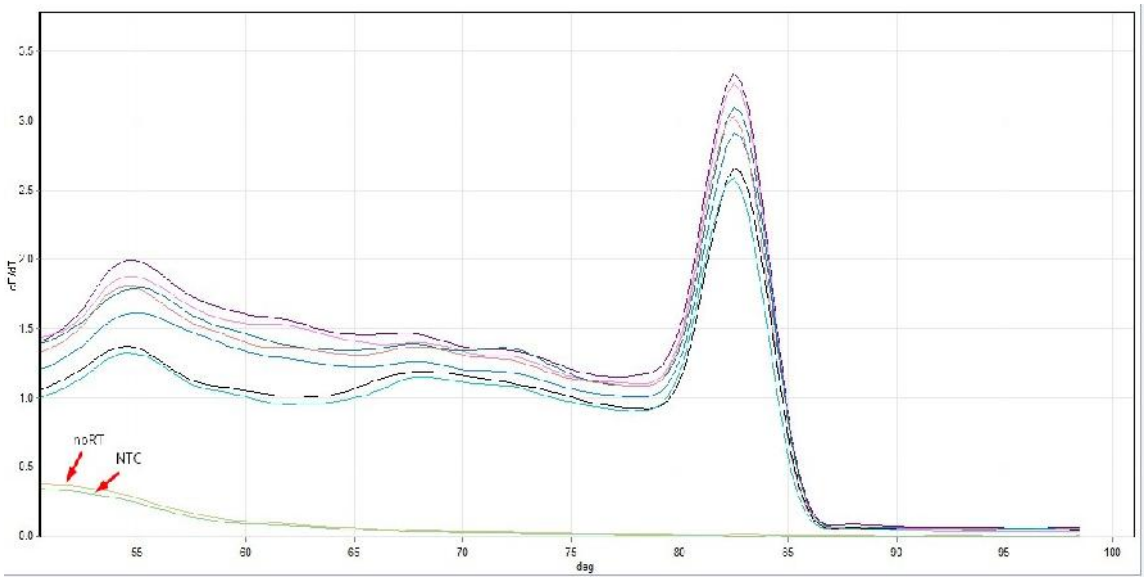

Figure C-2 *GAPDH* melt curve data analysis. All the standarts give peak approximately at 82.5ºC.

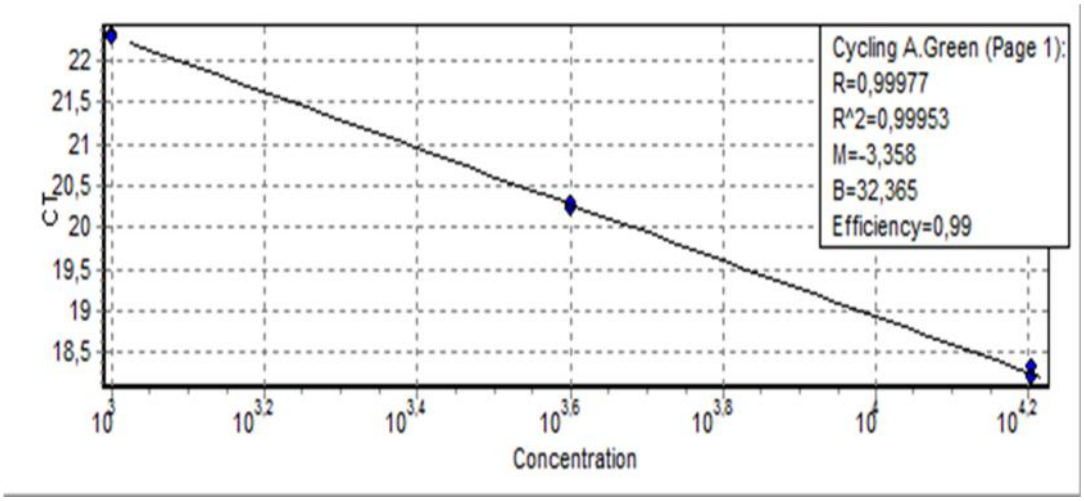

Figure C-3 *GAPDH* standard curve.

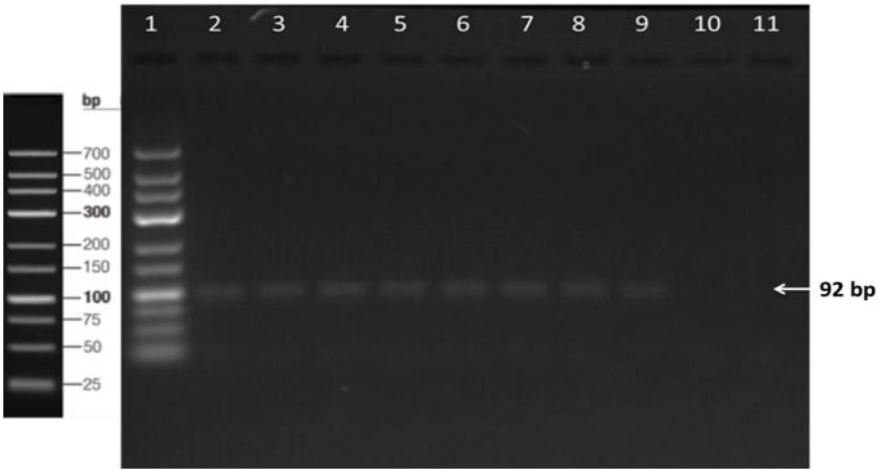

Figure C-4 Agarose gel image of *GAPDH* standard curve reaction. 1: DNA ladder, 2-4: 1/50 dilution, 5-7: 1/200 dilution, 8-9: 1/800 dilution, 10: noRT control, 11: NTC.

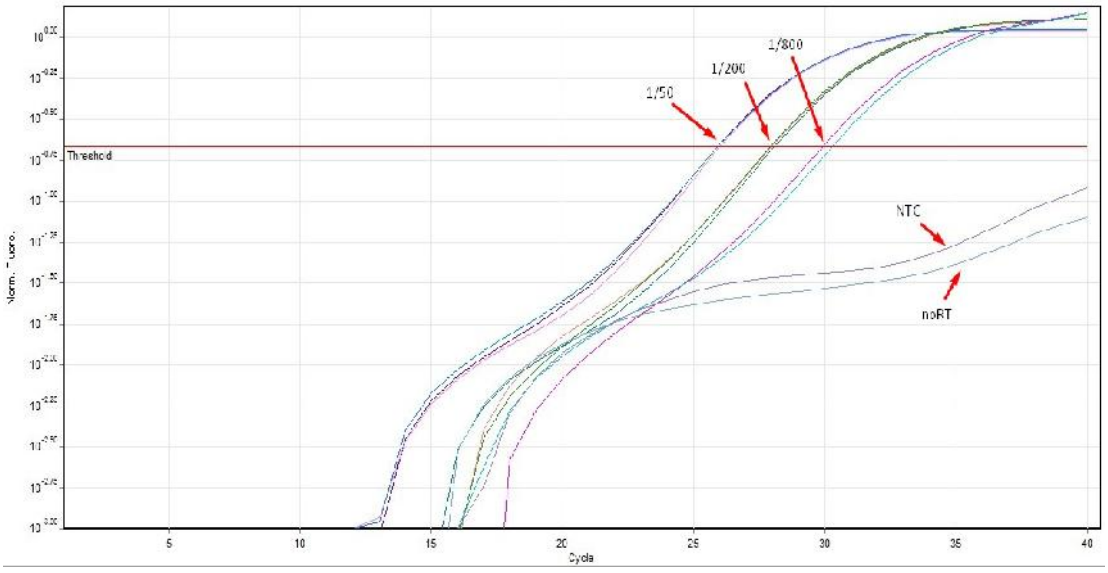

Figure C-5 *NPY* standard curve amplification data analysis.

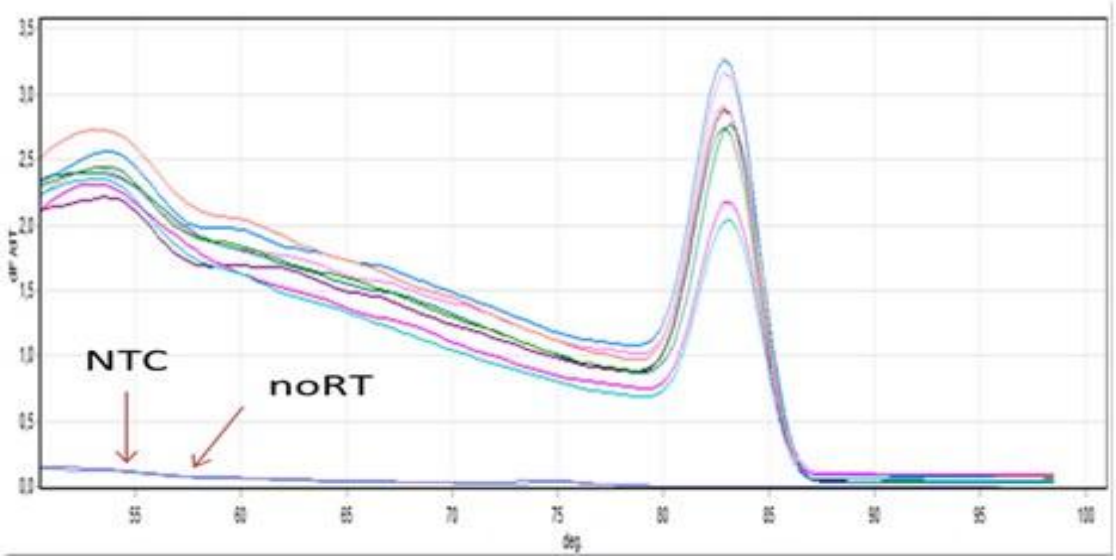

Figure C-6 *NPY* melt curve data analysis. All the standarts give peak approximately at 83ºC.

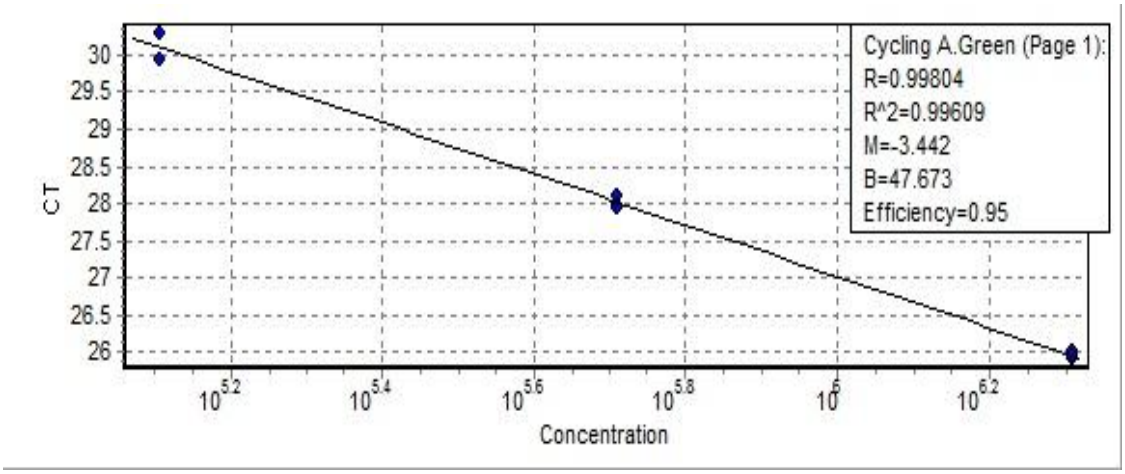

Figure C-7 *NPY* standard curve.

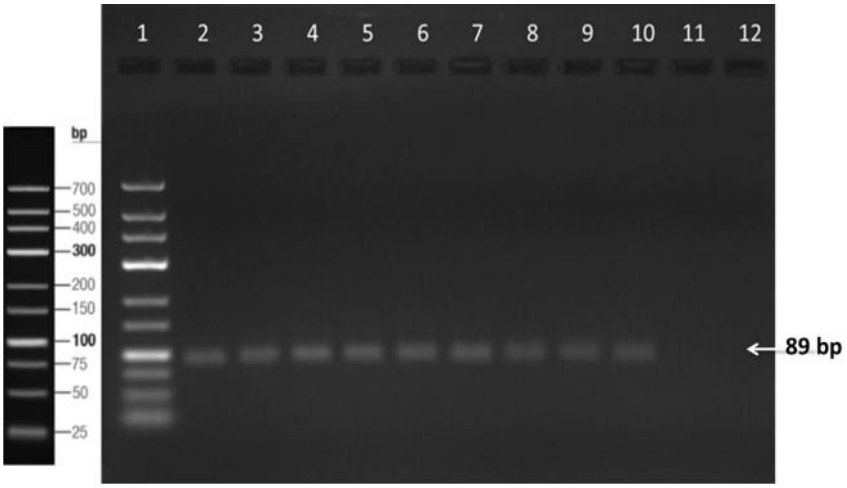

Figure C-8 Agarose gel image of *NPY* standard curve reaction. 1: DNA ladder, 2-4: 1/50 dilution, 5-7: 1/200 dilution, 8-10: 1/800 dilution, 11: noRT control, 12: NTC.

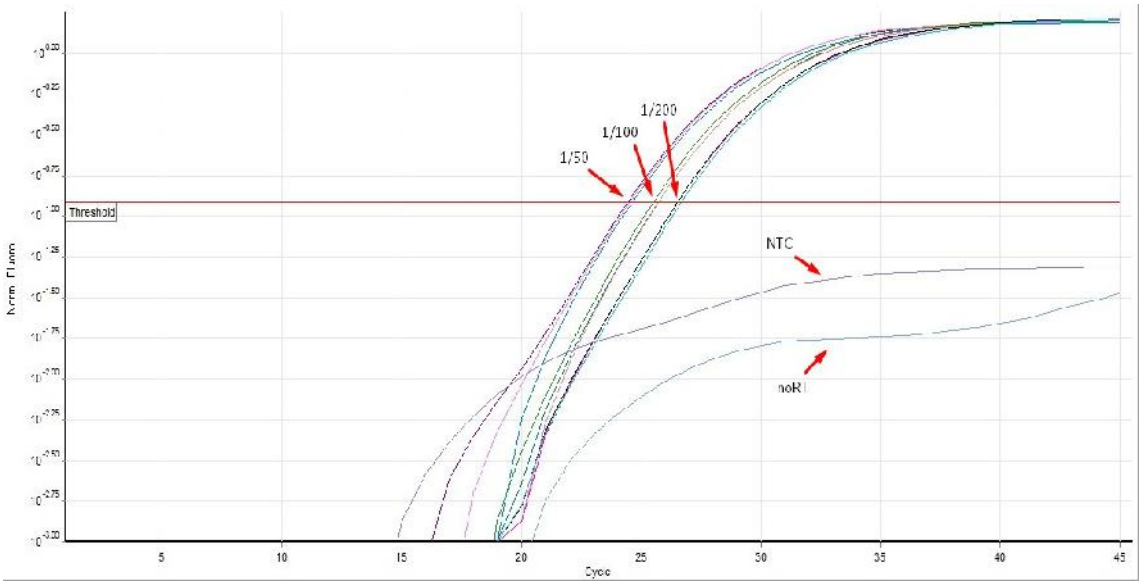

Figure C-9 *POMC* standard curve amplification data analysis.

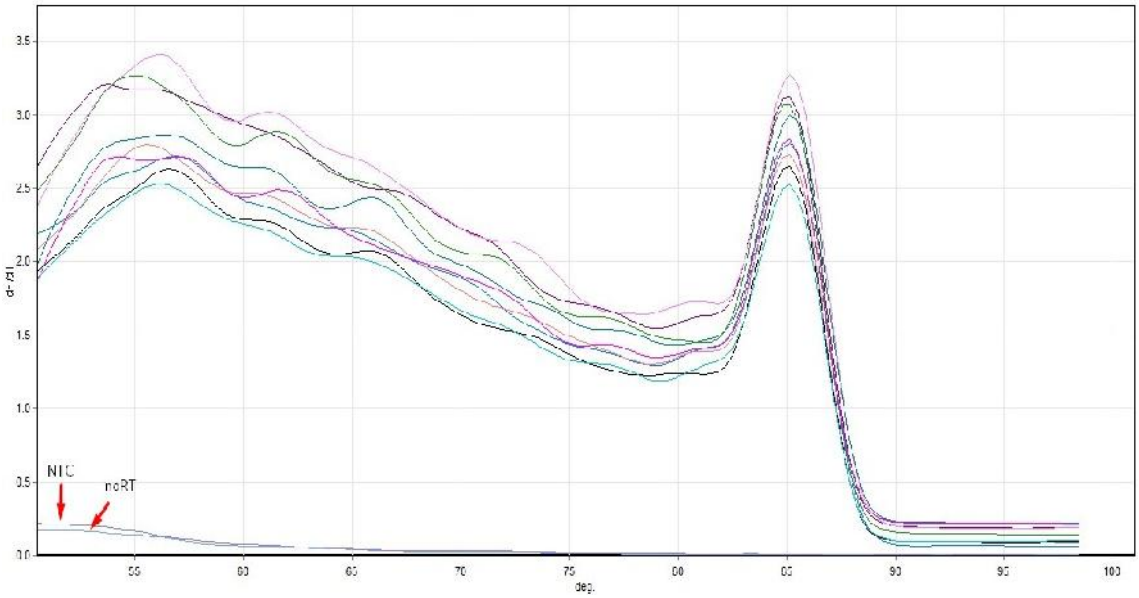

Figure C-10 *POMC* melt curve data analysis. All the standards give peak approximately at 85ºC.

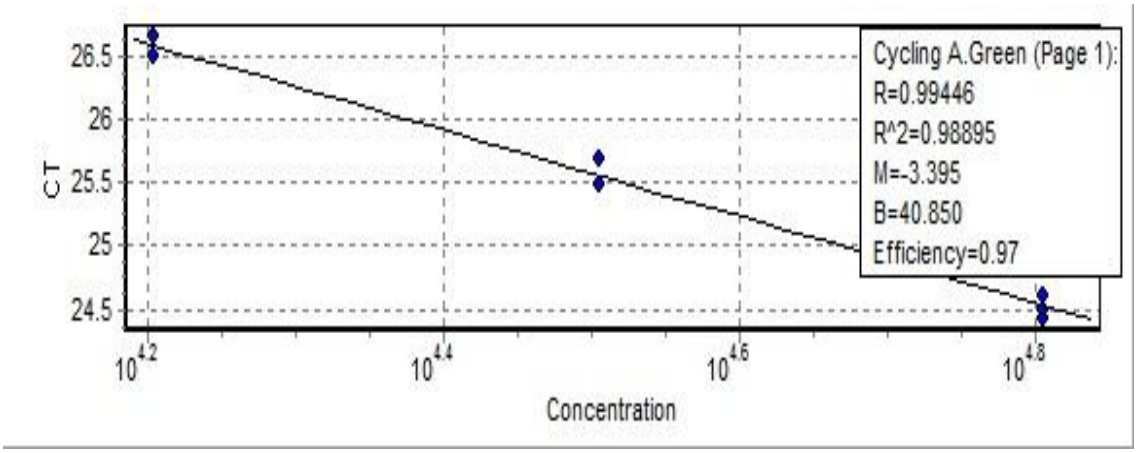

Figure C-11 *POMC* standard curve.

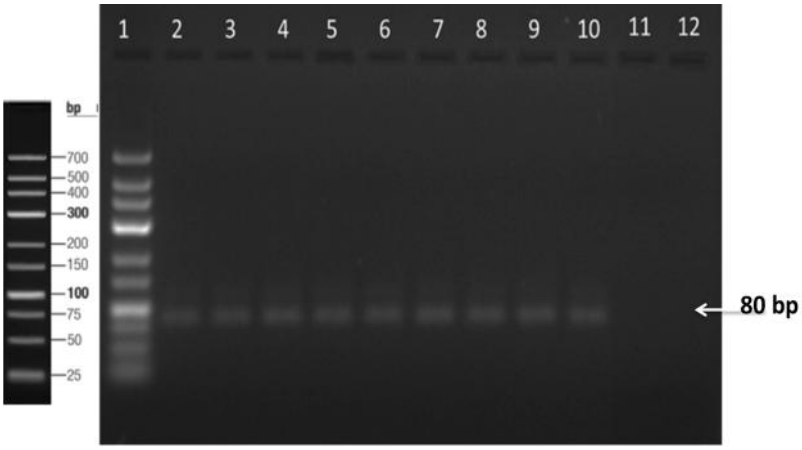

Figure C-12 Agarose gel image of *POMC* standard curve reaction. 1: DNA ladder, 2-4: 1/50 dilution, 5-7: 1/100 dilution, 8-10: 1/200 dilution, 11: noRT control, 12: NTC.

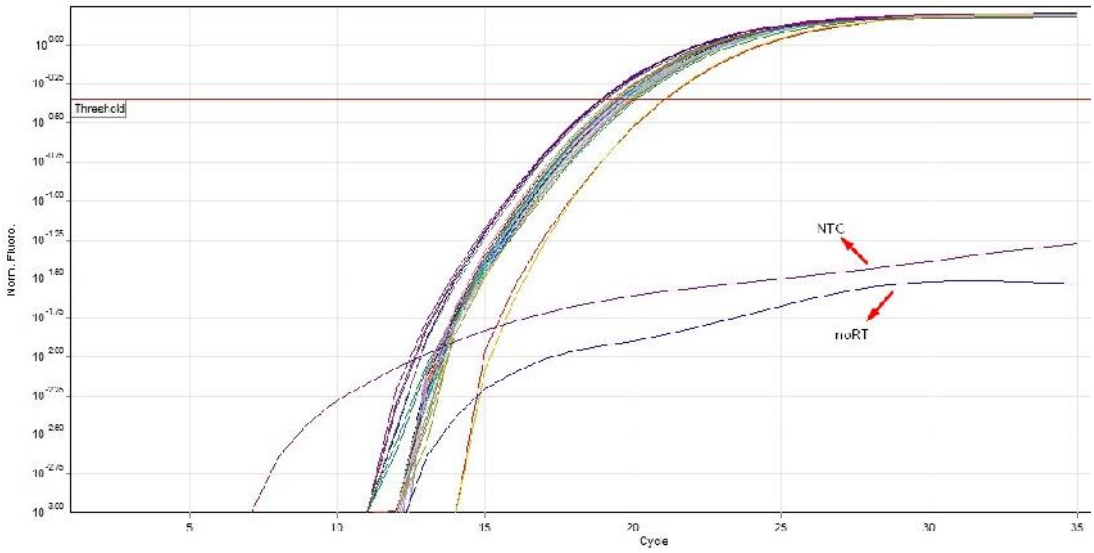

Figure C-13 *GAPDH* amplification data for control 1 group.

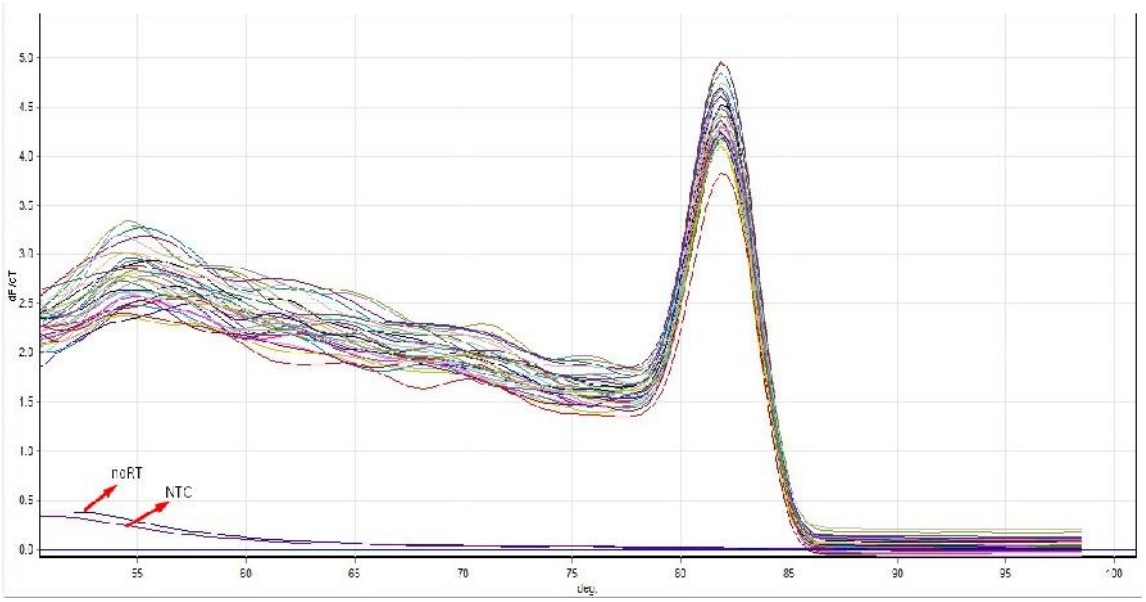

Figure C-14 *GAPDH* melt curve data for control 1 group.

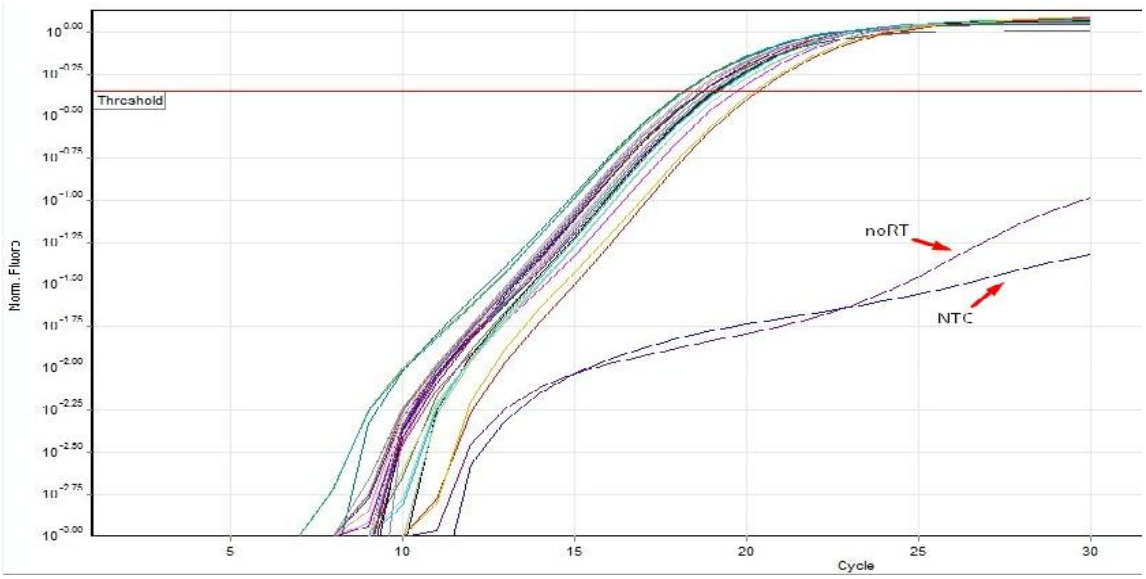

Figure C-15 *GAPDH* amplification data for control 2 group.

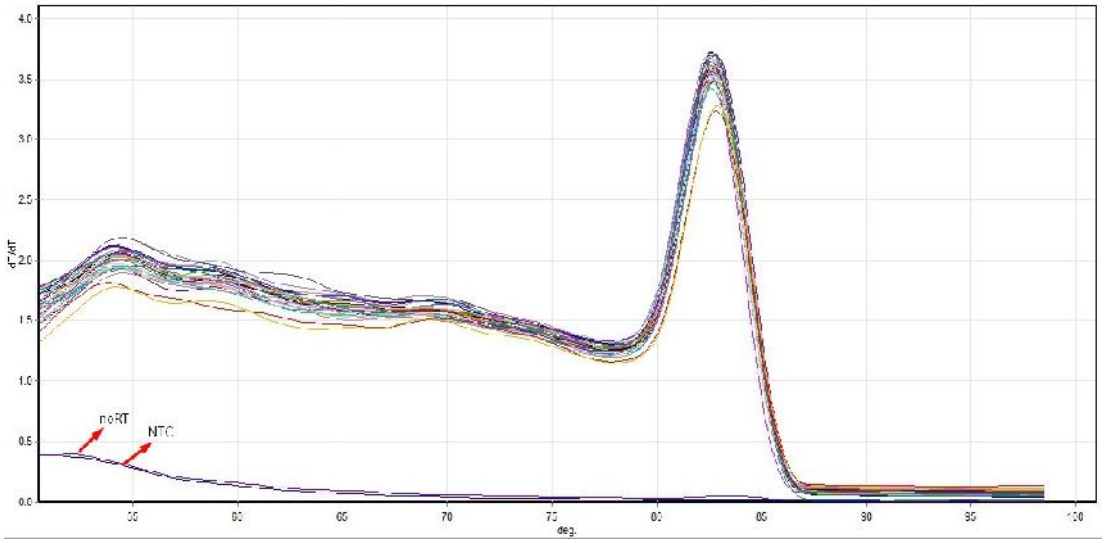

Figure C-16 *GAPDH* melt curve data for control 2 group.

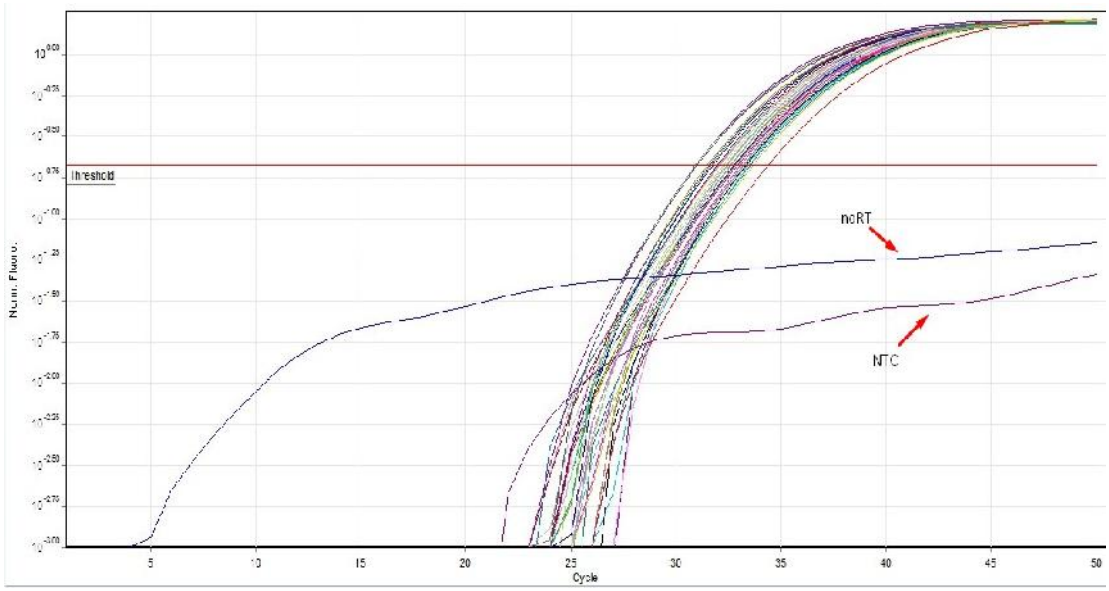

Figure C-17 *NPY* amplification data for control 1 group.

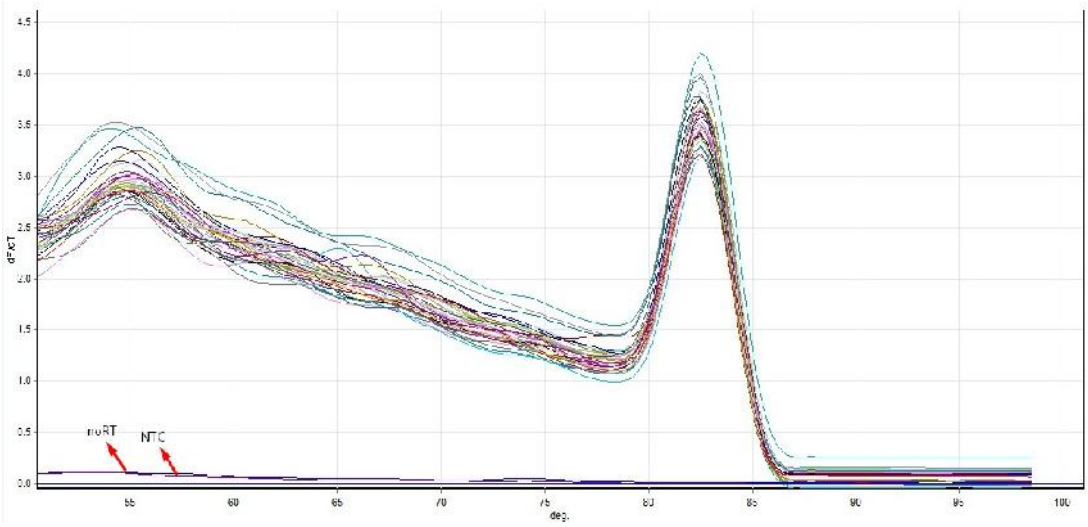

Figure C-18 *NPY* melt curve data for control 1 group.

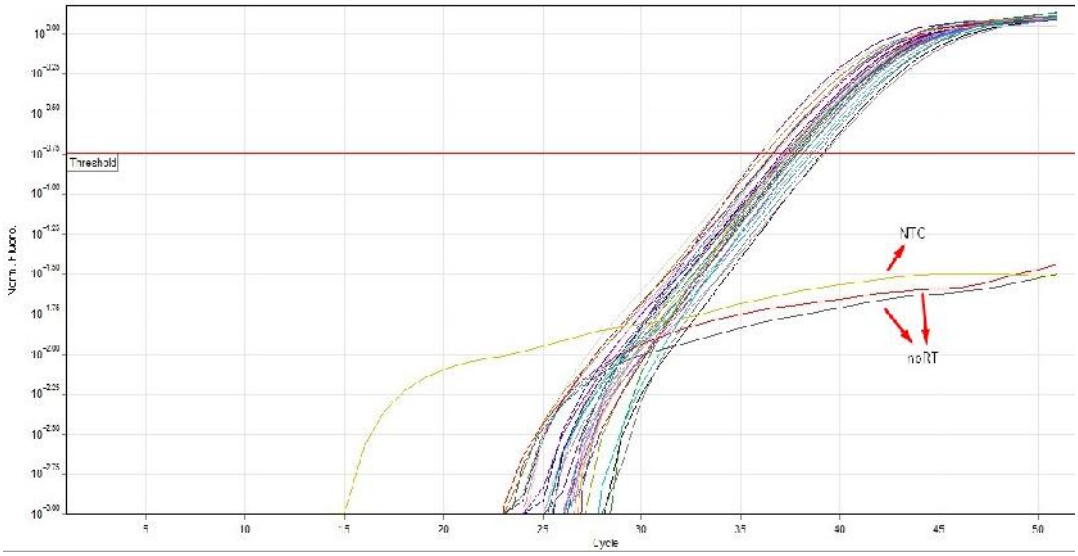

Figure C-19 *NPY* amplification data for control 2 group.

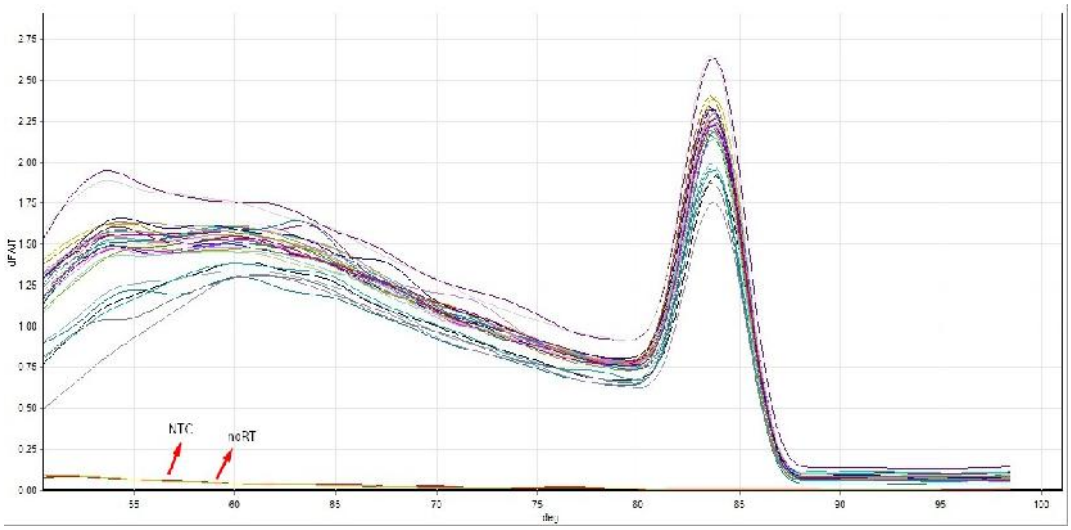

Figure C-20 *NPY* melt curve data for control 2 group.

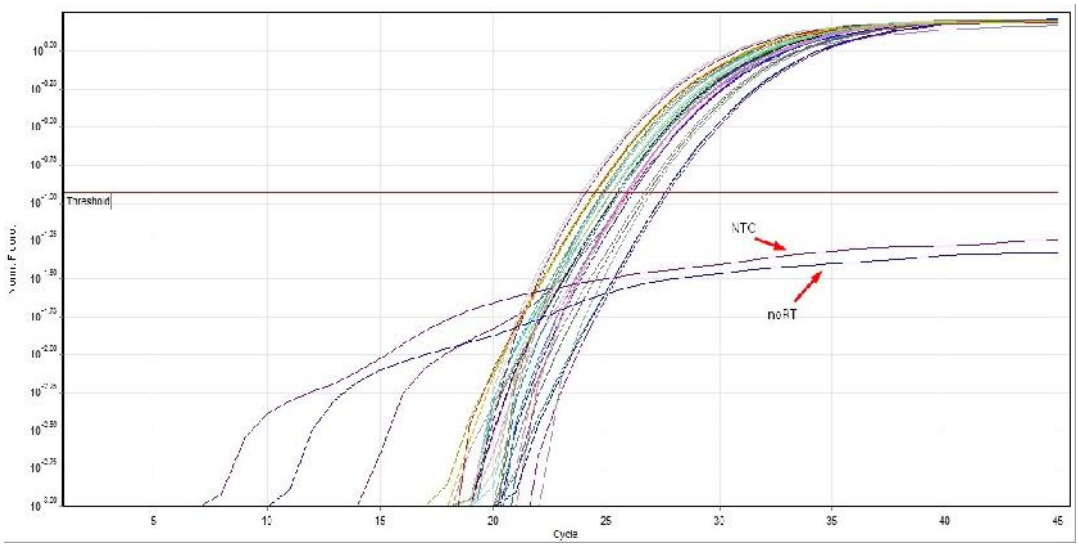

Figure C-21 *POMC* amplification data for control 1 group.

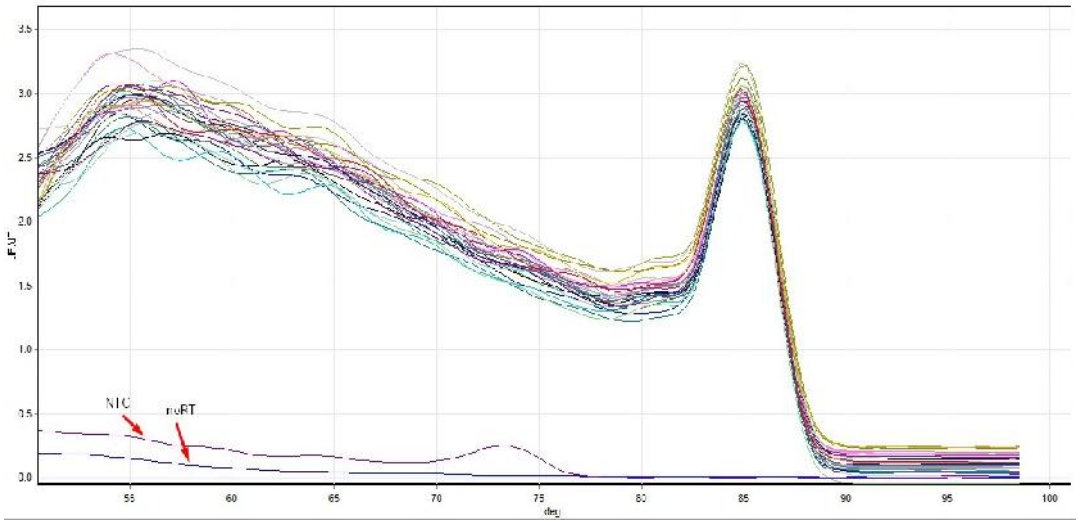

Figure C-22 *POMC* melt curve data for control 1 group.

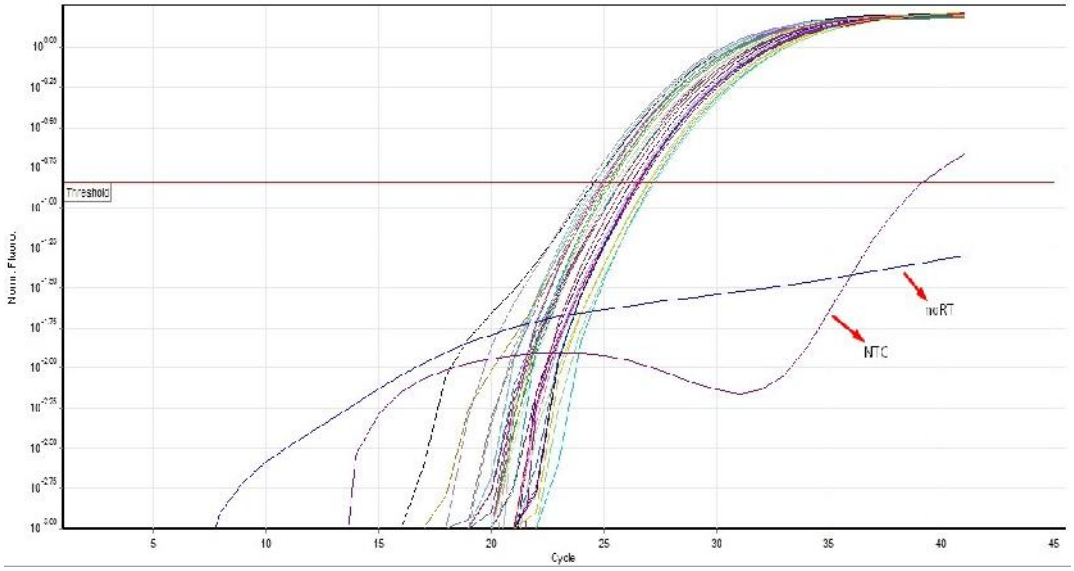

Figure C-23 *POMC* amplification data for control 2 group.

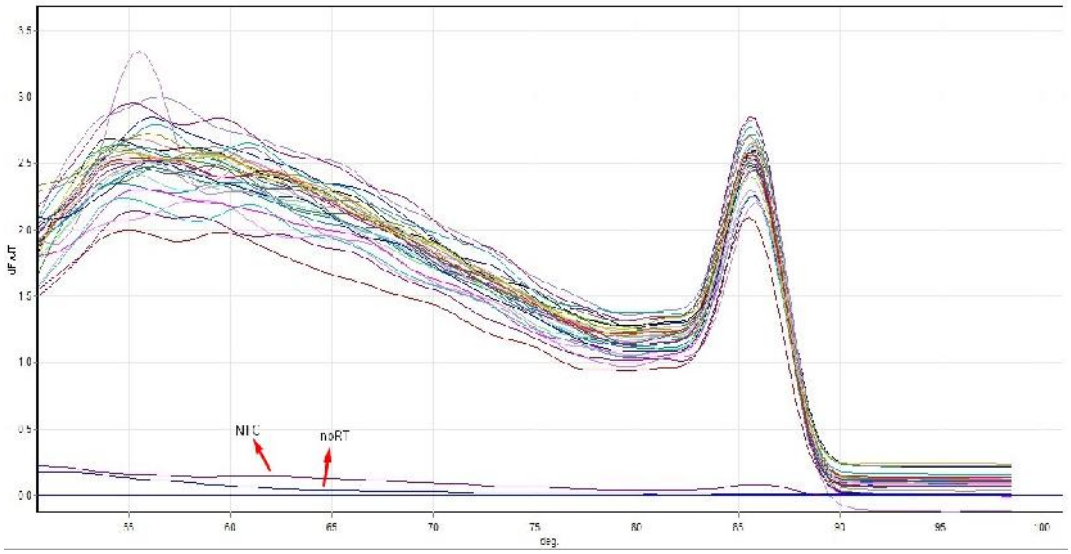

Figure C-24 *POMC* melt curve data for control 2 group.

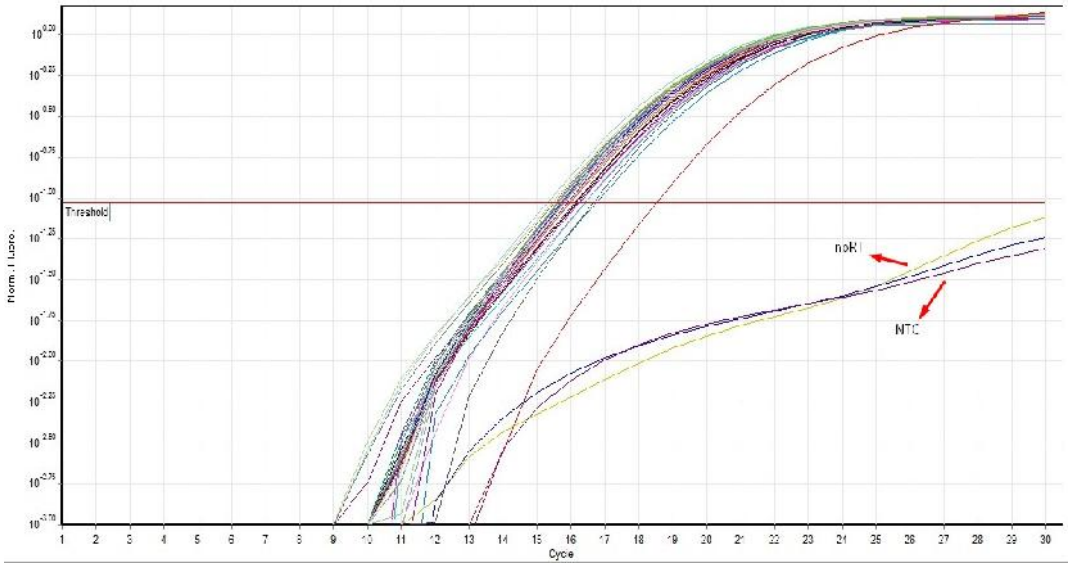

Figure C-25 *GAPDH* amplification data for arip 1 group.

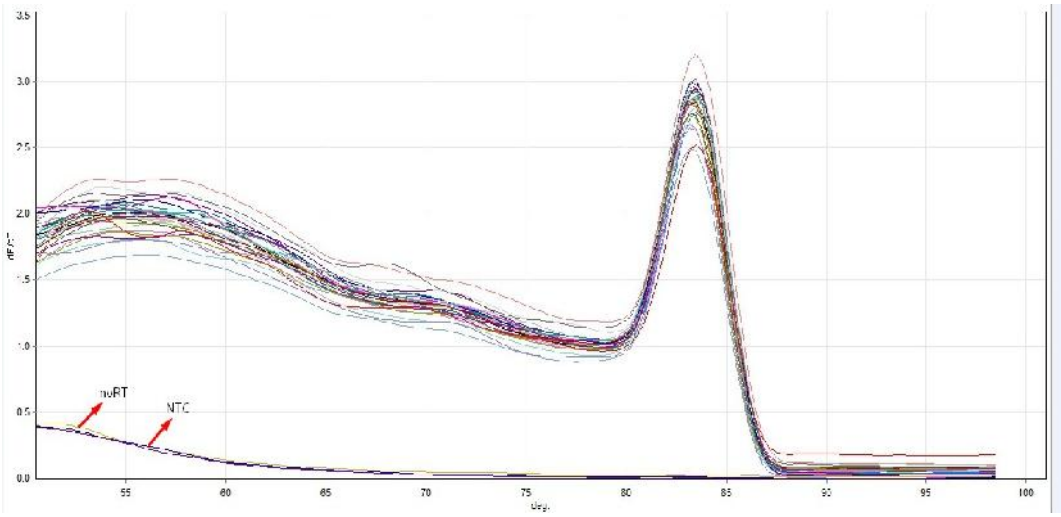

Figure C-26 *GAPDH* melt curve data for arip 1 group.

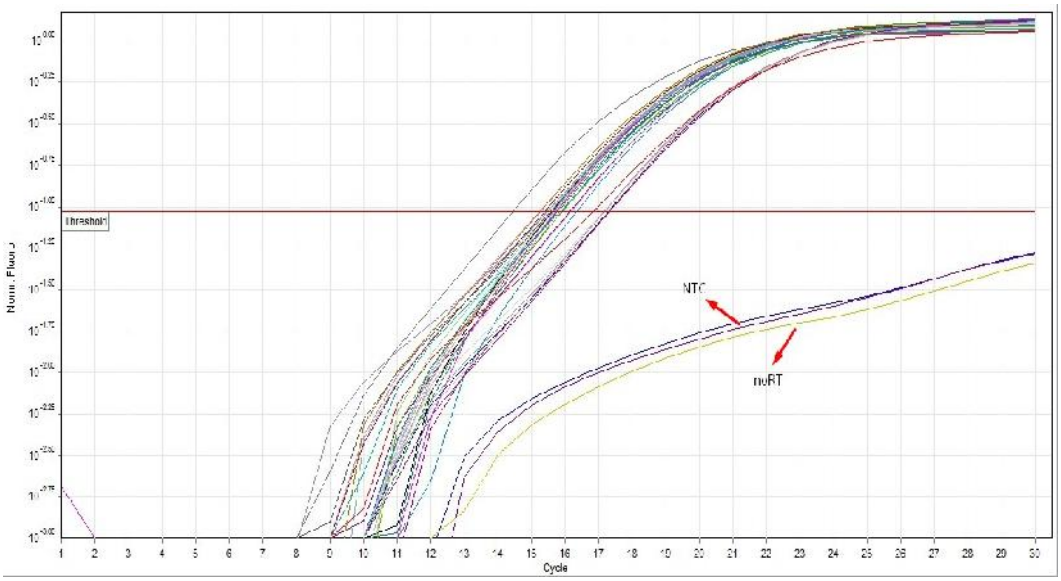

Figure C-27 *GAPDH* amplification data for arip 2 group.

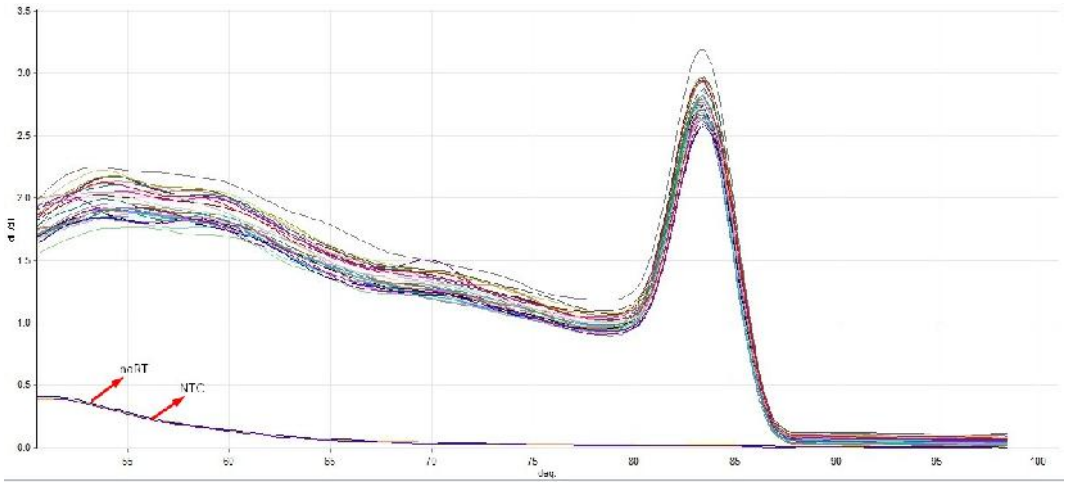

Figure C-28 *GAPDH* melt curve data for arip 2 group.

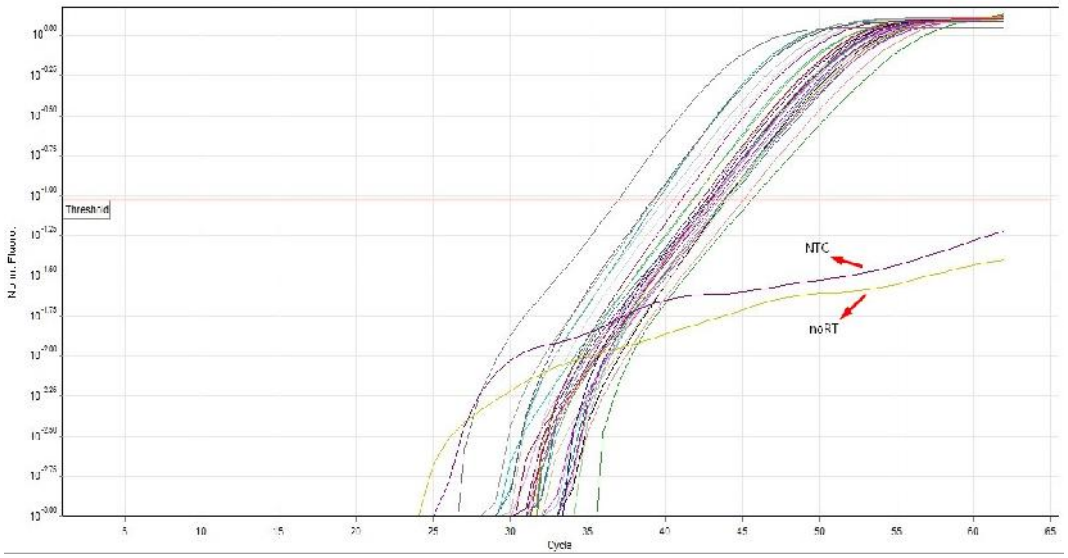

Figure C-29 *NPY* amplification data for arip 1 group.

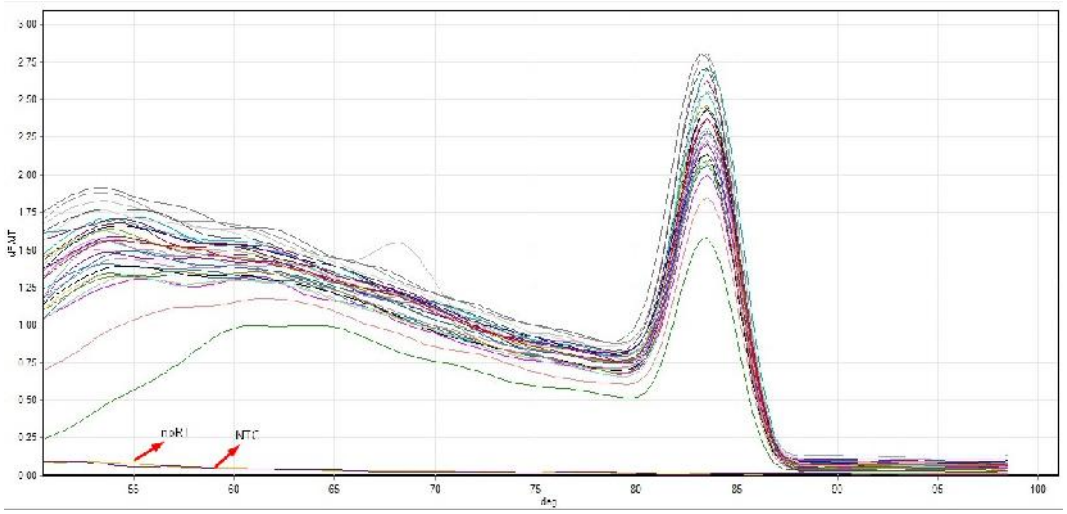

Figure C-30 *NPY* melt curve data for arip 1 group.

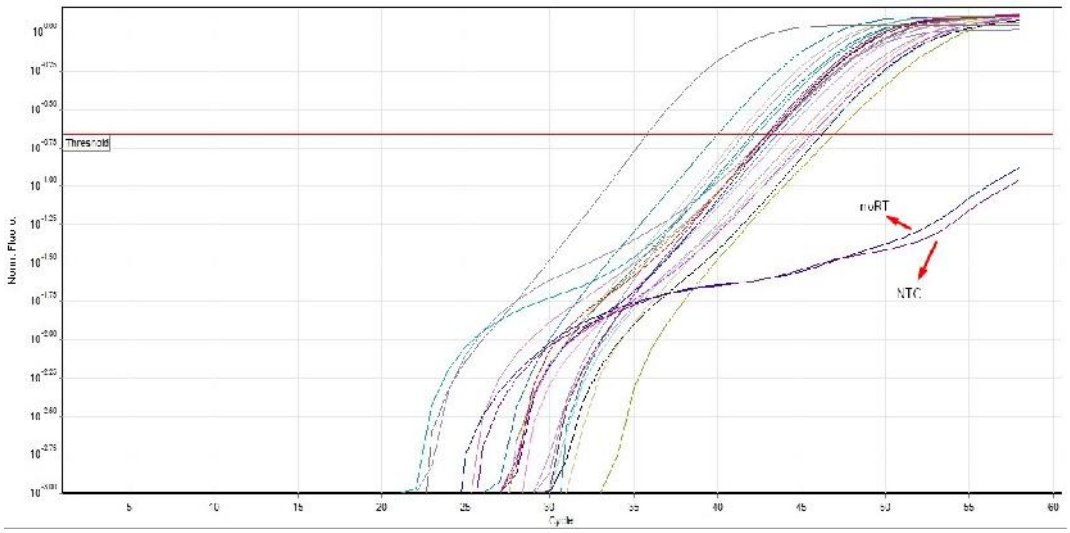

Figure C-31 *NPY* amplification data for arip 2 group.

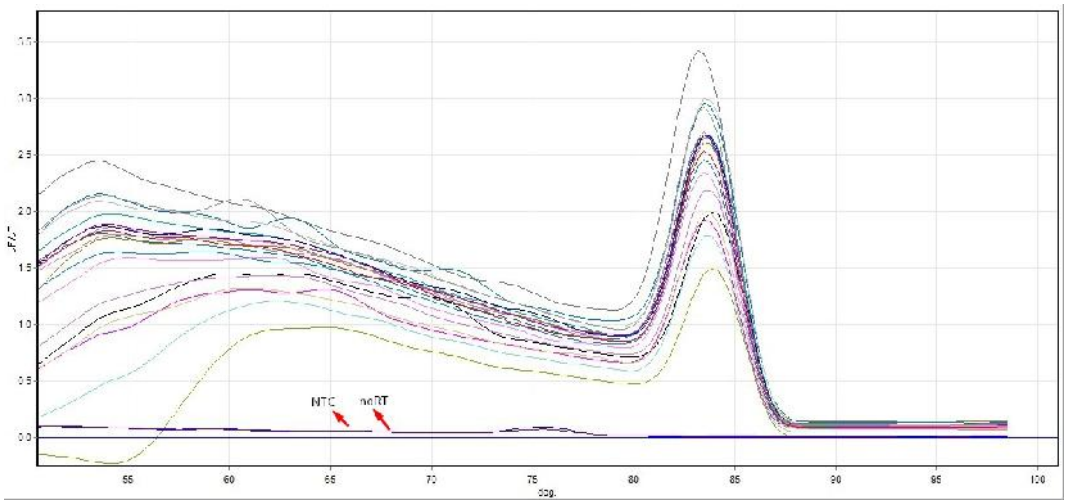

Figure C-32 *NPY* melt curve data for arip 2 group.

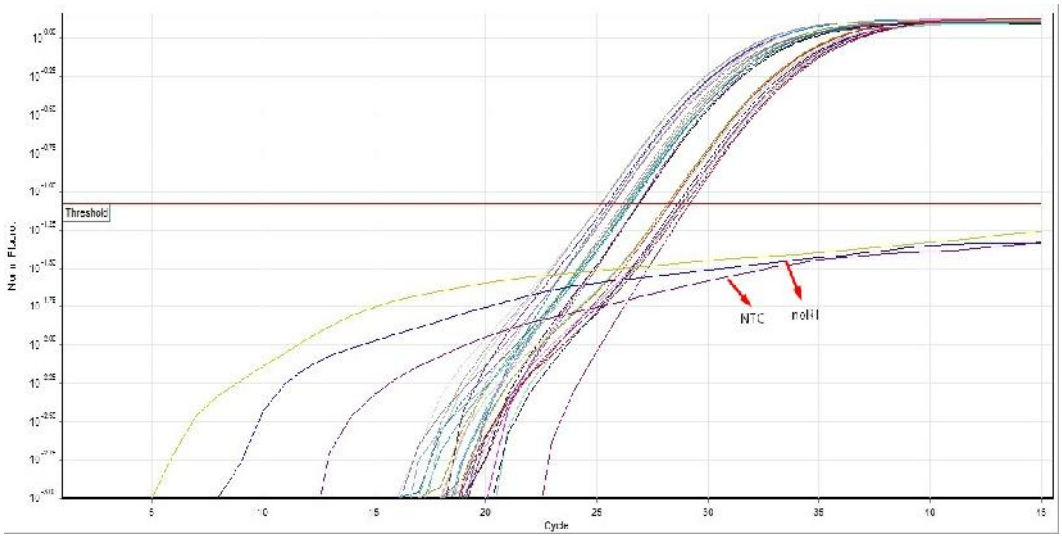

Figure C-33 *POMC* amplification data for arip 1 group.

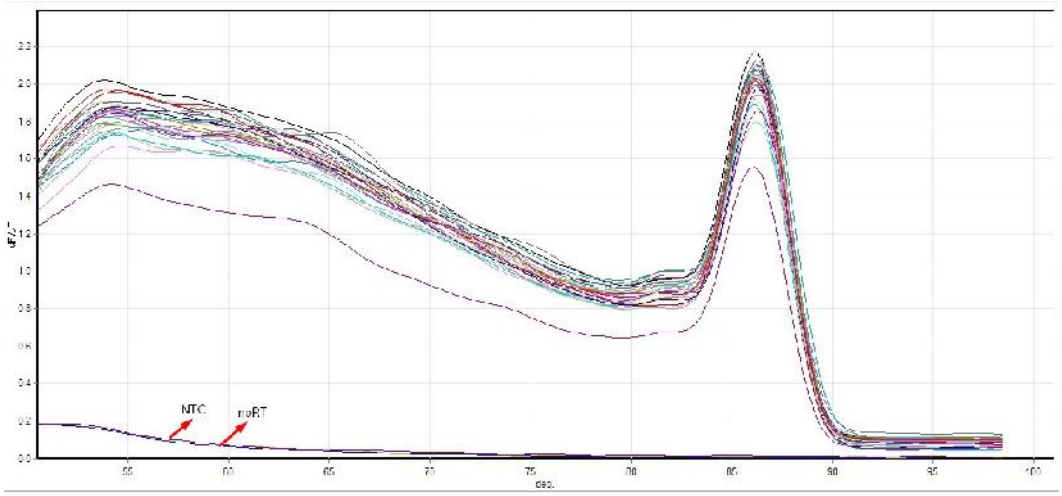

Figure C-34 *POMC* melt curve data for arip 1 group.

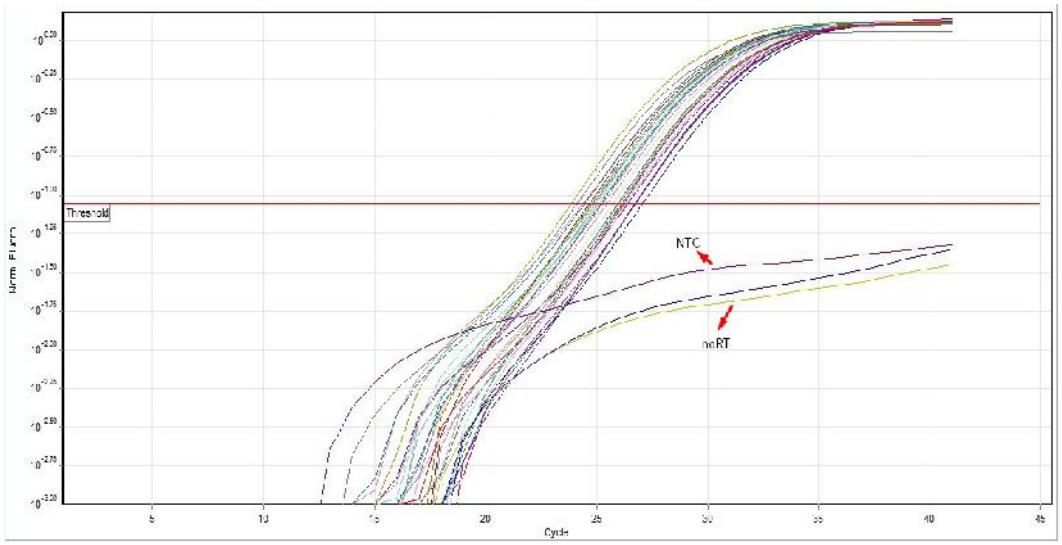

Figure C-35 *POMC* amplification data for arip 2 group.

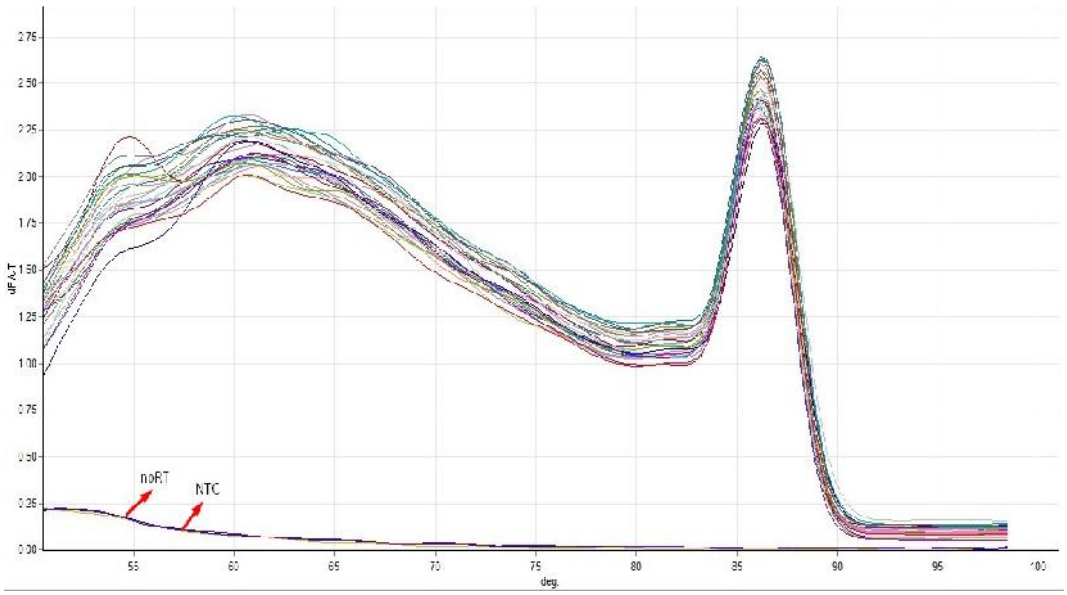

Figure C-36 *POMC* melt curve data for arip 2 group.

Table C-1 Mean Ct values.

Mean *GAPDH* Ct values			
CTRL 1	CTRL 2	ARIP 1	ARIP 2
19.86	19.04	16.45	16.20
19.66	19.12	16.27	15.83
20.00	19.33	15.44	15.65
20.09	19.41	15.67	15.59
19.70	18.51	16.01	15.52
19.53	18.75	15.73	15.30
19.30	18.21	15.79	15.84
19.40	18.71	15.75	17.30
19.08	18.90		17.16
19.52			
Mean *POMC* Ct values			
CTRL 1	CTRL 2	ARIP 1	ARIP 2
26.09	26.41	25.58	26.51
25.79	25.67	26.71	26.01
25.49	24.83	28.47	25.02
25.23	27.10	26.30	25.23
25.12	24.53	28.66	24.63
25.87	26.46	26.44	24.41
24.74	25.18	28.87	26.85
27.66	26.51	25.18	25.97
24.03	25.57		
26.84			
Mean *NPY* Ct values			
CTRL 1	CTRL 2	ARIP 1	ARIP 2
32.83	37.51	43.26	43.76
33.33	36.60	44.90	42.08
32.51	37.51	43.19	45.89
33.62	38.46	43.59	45.61
32.54	37.24	43.22	43.94
33.17	38.34	42.90	43.23
32.52	36.49	41.35	43.08
31.61	38.10	42.33	43.06
31.85	37.37		41.42
32.39			

APPENDIX D

IDENTIFICATION OF RATS

Table D-1 Identification of rat groups.

Group IDs	CTRL 1	CTRL 2	ARIP 1	ARIP 2
Rat IDs	C1R1 C1R2 C1R3 C1R4 C2R1 C2R2 C2R3 C3R1 C3R2 C3R3	C4R1 C4R2 C4R3 C4R4 C5R1 C5R2 C5R3 C6R1 C6R2 C6R3	C17R1 C17R2 C17R3 C18R1 C18R2 C18R3 C19R1 C19R3 C19R4	C16R1 C16R2 C16R3 C16R4 C20R1 C20R2 C20R3 C23R1 C23R2

APPENDIX E

RNA CONCENTRATIONS

Table E-1 RNA concentrations, A_{260}/A_{280} and A_{260}/A_{230} ratios of control groups after DNase treatment and cleanup protocol.

Group ID	Sample ID	Concentration (ng/µL)	OD_{260}/OD_{280}	OD_{260}/OD_{230}
CTRL1	C1R1	664.8	2.08	2.18
	C1R2	431.9	2.02	1.98
	C1R3	514.7	2.10	2.00
	C1R4	570.9	2.10	2.05
	C2R1	564.5	2.11	2.13
	C2R2	591.8	2.09	2.12
	C2R3	428.7	2.02	2.13
	C3R1	405.0	2.04	2.18
	C3R2	594.7	2.08	2.05
	C3R3	559.1	2.10	2.16
CTRL2	C4R1	617.8	2.13	2.14
	C4R2	1352.9	2.11	2.02
	C4R3	619.7	2.14	1.60
	C4R4	668.2	2.10	2.10

Table E-1 RNA concentrations, A_{260}/A_{280} and A_{260}/A_{230} ratios of control groups after DNase treatment and cleanup protocol (Continued).

Group ID	Sample ID	Concentration (ng/µL)	OD_{260}/OD_{280}	OD_{260}/OD_{230}
CTRL2	**C5R1**	490.9	2.12	1.84
	C5R2	639.3	2.09	2.22
	C5R3	842.8	2.09	2.20
	C6R1	803.8	2.08	2.15
	C6R2	303.8	1.99	1.68
	C6R3	494.1	2.07	2.01

Table E-2 RNA concentrations, A_{260}/A_{280} and A_{260}/A_{230} ratios of experimental groups after DNase treatment and cleanup protocol.

Group ID	Sample ID	Concentration (ng/µL)	OD_{260}/OD_{280}	OD_{260}/OD_{230}
ARIP1	**C17R1**	467.7	2.12	2.17
	C17R2	492.9	2.12	1.86
	C17R3	345.4	2.04	1.98
	C18R1	569.7	2.07	1.81
	C18R2	387.5	2.08	2.14
	C18R3	623.2	2.10	1.93
	C19R1	443.2	2.07	1.89
	C19R3	486.0	2.08	1.92
	C19R4	368.2	2.02	1.87

Table E-2 RNA concentrations, A_{260}/A_{280} and A_{260}/A_{230} ratios of experimental groups after DNase treatment and cleanup protocol (Continued).

Group ID	Sample ID	Concentration (ng/µL)	OD_{260}/OD_{280}	OD_{260}/OD_{230}
ARIP2	**C16R1**	397.5	2.11	1.66
	C16R2	516.0	2.11	1.78
	C16R3	486.4	2.12	1.83
	C16R4	526.9	2.09	1.81
	C20R1	620.0	2.11	1.93
	C20R2	566.3	2.12	1.76
	C20R3	512.2	2.11	1.86
	C23R1	384.5	2.03	1.65
	C23R2	374.4	2.06	2.08

APPENDIX F

AGAROSE GEL IMAGES OF RNA SAMPLES

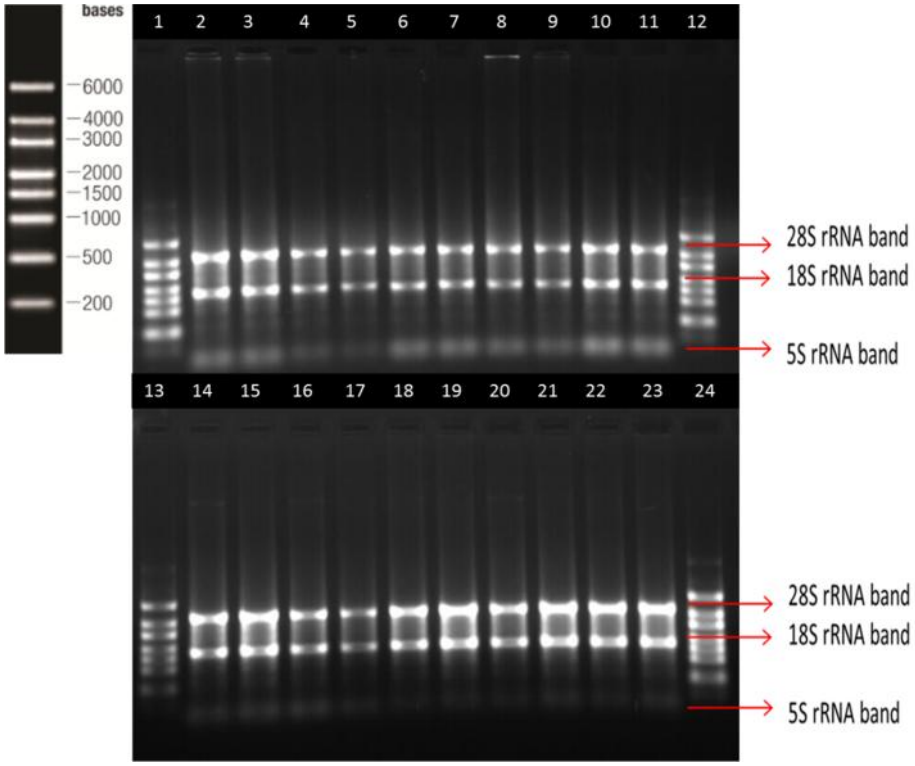

Figure F-1 Total RNA gel electrophoresis image of control 1 before and after DNase treatment. RNA ladder bands' sizes are depicted on the left. (1, 12, 13 and 24: RNA ladder, 2-3: C1R1, 4-5: C1R2, 6-7: C1R3, 8-9: C1R4, 10-11: C2R1, 14-15: C2R2, 16-17: C2R3, 18-19: C3R1, 20-21: C3R2. 22-23: C3R3).

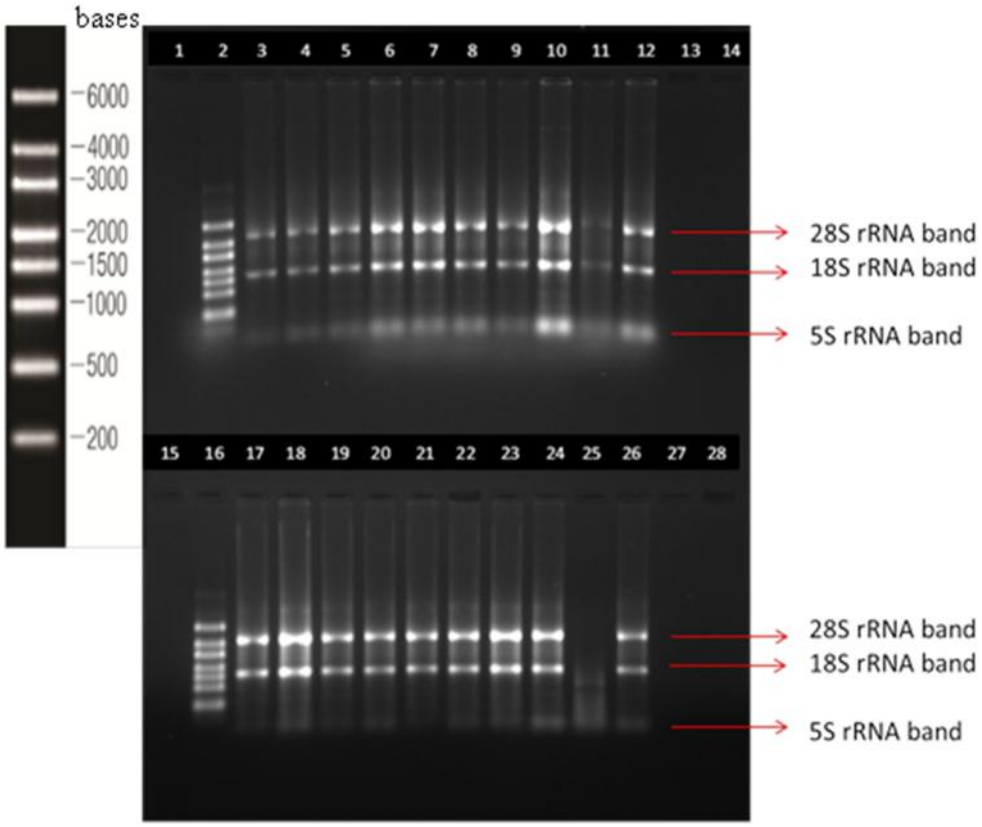

Figure F-2 Total RNA gel electrophoresis image of control 2 before and after DNase treatment. RNA ladder bands' sizes are depicted on the left. (2: RNA ladder, 3: C4R1, 4: C4R2, 5: C4R3, 6: C4R4, 7: C5R1, 8: C5R2, 9: C5R3, 10: C6R1, 11: C6R2. 12: C6R3, 16: RNA ladder, 17: C4R1, 18: C4R2, 19: C4R3, 20: C4R4, 21: C5R1, 22: C5R2, 23: C5R3, 24: C6R1, 25: C6R2, 26: C6R3, 13 and 27: nuclease free water as a blank).

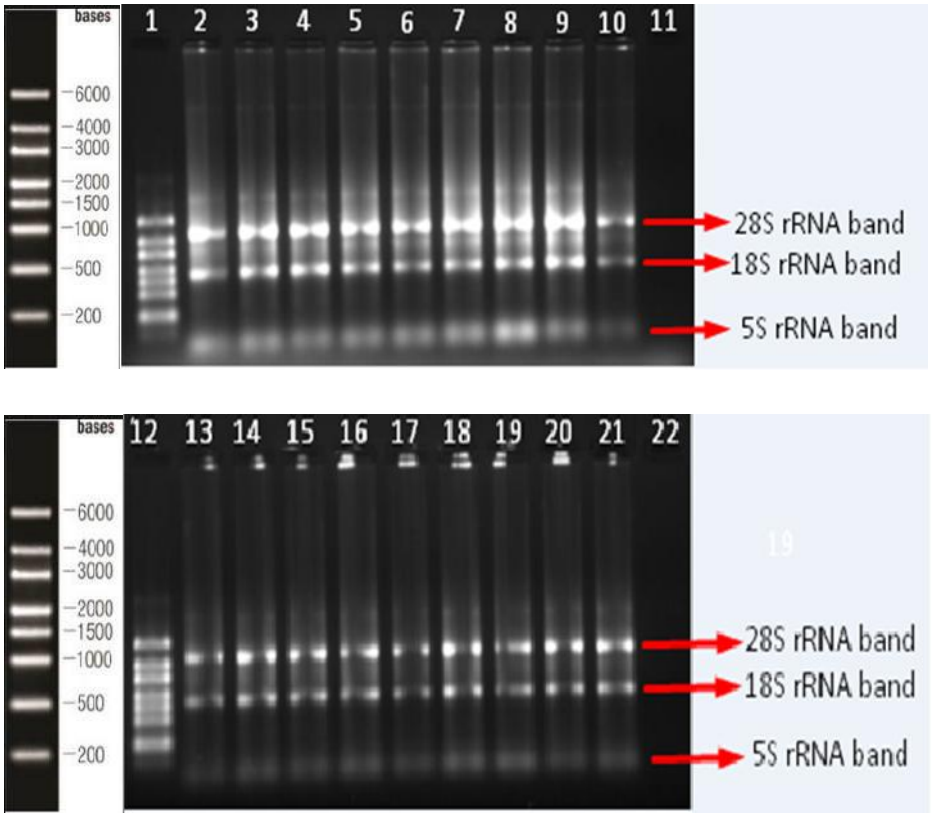

Figure F-3 Total RNA gel electrophoresis image of arip 1 before and after DNase treatment. RNA ladder bands' sizes are depicted on the left. (1: RNA ladder, 2: C17R1, 3: C17R2, 4: C17R3, 5: C18R1, 6: C18R2, 7: C18R3, 8: C19R1, 9: C19R3, 10: C19R4. 11: blank, 12: RNA ladder, 13: C17R1, 14: C17R2, 15: C17R3, 16: C18R1, 17: C18R2, 18: C18R3, 19: C19R1, 20: C19R3, 21: C19R4, 22: blank).

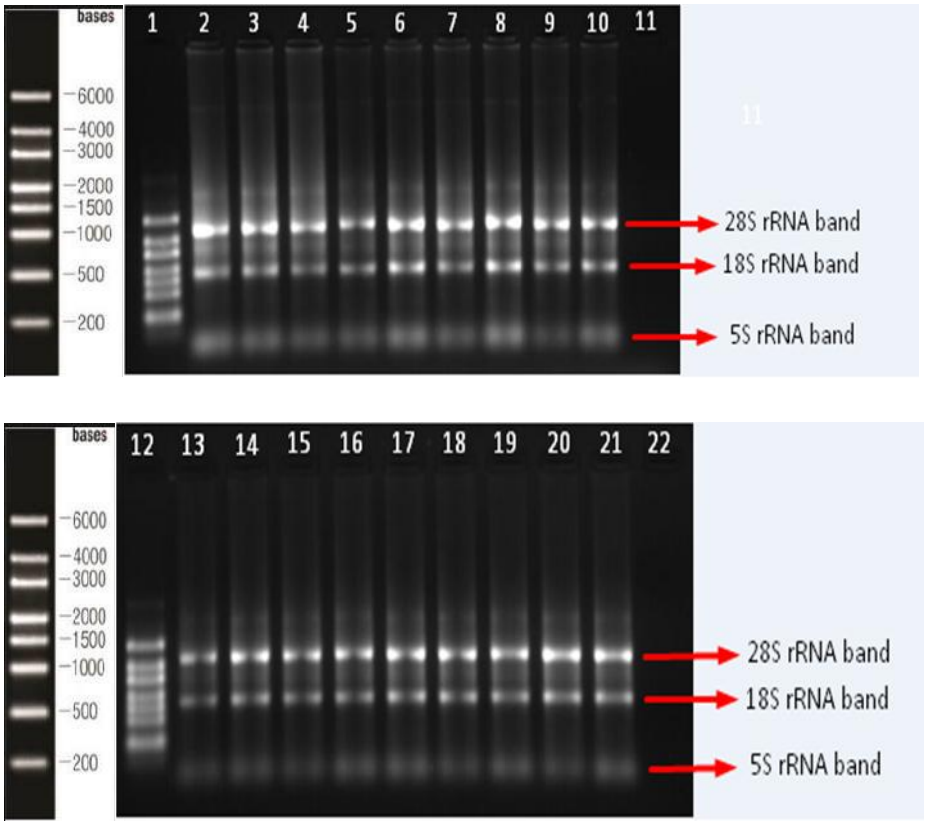

Figure F-4 Total RNA gel electrophoresis image of arip 2 before and after DNase treatment. RNA ladder bands' sizes are depicted on the left. (1: RNA ladder, 2: C16R1, 3: C16R2, 4: C16R3, 5: C16R4, 6: C20R1, 7: C20R2, 8: C20R3, 9: C23R1, 10: C23R2, 11: blank, 12: RNA ladder, 13: C16R1, 14: C16R2, 15: C16R3, 16: C16R4, 17: C20R1, 18: C20R2, 19: C20R3, 20: C23R1, 21: C23R2, 22: blank).